Canad. J. Math. Vol. 75 (4), 2023 pp. 1226–1271
http://dx.doi.org/10.4153/S0008414X22000323

Loops in the fundamental group of $\mathrm{Symp}(\mathbb{CP}^2\#5\overline{\mathbb{CP}}^2,\omega)$ which are not represented by circle actions

Sílvia Anjos, Miguel Barata, Martin Pinsonnault, and Ana Alexandra Reis

Abstract. We study generators of the fundamental group of the group of symplectomorphisms $\mathrm{Symp}(\mathbb{CP}^2\#5\overline{\mathbb{CP}}^2,\omega)$ for some particular symplectic forms. It was observed by Kędra (2009, *Archivum Mathematicum* 45) that there are many symplectic 4-manifolds (M,ω), where M is neither rational nor ruled, that admit no circle action and $\pi_1(\mathrm{Ham}(M,\omega))$ is nontrivial. On the other hand, it follows from Abreu and McDuff (2000, *Journal of the American Mathematical Society* 13, 971–1009), Anjos and Eden (2019, *Michigan Mathematical Journal* 68, 71–126), Anjos and Pinsonnault (2013, *Mathematische Zeitschrift* 275, 245–292), and Pinsonnault (2008, *Compositio Mathematica* 144, 787–810) that the fundamental group of the group $\mathrm{Symp}_h(\mathbb{CP}^2\#k\overline{\mathbb{CP}}^2,\omega)$, of symplectomorphisms that act trivially on homology, with $k\leq 4$, is generated by circle actions on the manifold. We show that, for some particular symplectic forms ω, the set of all Hamiltonian circle actions generates a proper subgroup in $\pi_1(\mathrm{Symp}_h(\mathbb{CP}^2\#5\overline{\mathbb{CP}}^2,\omega))$. Our work depends on Delzant classification of toric symplectic manifolds, Karshon's classification of Hamiltonian S^1-spaces, and the computation of Seidel elements of some circle actions.

1 Introduction

Let (M,ω) be a closed simply connected symplectic manifold. The symplectomorphism group $\mathrm{Symp}(M,\omega)$, equipped with the standard C^∞-topology, is an infinite-dimensional Fréchet Lie group. In general, symplectomorphism groups are viewed as intermediate objects between Lie groups and general groups of diffeomorphisms. Of course, this philosophy can be understood in many different ways. One interesting question is to compare the homotopy types of various symplectomorphism groups with those of compact Lie groups, and see to what extend their homotopical and algebraic properties are related. For instance, recall that if G is a compact Lie group,

Received by the editors October 9, 2019; revised May 3, 2022; accepted June 19, 2022.
Published online on Cambridge Core June 30, 2022.
The first author is partially supported by FCT/Portugal through projects UID/MAT/04459/2019 and PTDC/MAT-PUR/29447/2017. The third author is partially supported by NSERC Discovery Grant RGPIN-2020-06428. All authors except the third are supported by the Calouste Gulbenkian Foundation through the program "New Talents in Mathematics."
AMS subject classification: **53D35**, 57R17, 57S05, 57T20.
Keywords: symplectic geometry, symplectomorphism group, fundamental group, Hamiltonian circle actions.

then any element of its fundamental group $\pi_1(G)$ is represented by a continuous homomorphism $S^1 \to G$. Therefore, it is natural to ask whether the same holds for symplectomorphism groups.

Question 1.1 Suppose that $\pi_1(\mathrm{Symp}(M,\omega))$ is nontrivial. Is every element represented by a continuous homomorphism $S^1 \mapsto \mathrm{Symp}(M,\omega)$ (i.e., a circle action on M)? If not, can we characterize homotopy classes that are represented by circle actions? ∎

In [13], Kędra showed that the answer to the first part of the question is negative in general.

Theorem 1.2 [13] *Let* (M,ω) *be a symplectic blowup (in a small ball) of a closed simply connected Kähler surface, which is neither a rational nor a ruled surface up to the blowup. Then* (M,ω) *admits no symplectic circle action, although* $\pi_1(\mathrm{Symp}(M,\omega))$ *is nontrivial.*

A concrete example is obtained by taking a K3 surface with any symplectic form. Another type of example was found by Buse in her work on symplectomorphism groups of irrational ruled surfaces [6, Proposition 3.3]. More precisely, although $\mathbb{T}^2\times S^2$ admits Hamiltonian circle actions, she showed that there is an element $\gamma\in\pi_1(\mathrm{Ham}(\mathbb{T}^2\times S^2))$ for which the rational Samelson product $[\gamma,\gamma]_{\mathbb{Q}}$ does not vanish, which implies that γ cannot be represented by such an action.

In the present paper, we consider the symplectic rational surfaces $(\mathbb{CP}^2\# n\overline{\mathbb{CP}}^2,\omega)$. For $1\le n\le 5$, the topological group $\mathrm{Symp}_h(\mathbb{CP}^2\# n\overline{\mathbb{CP}}^2,\omega)$ of symplectomorphisms that act trivially on homology has been studied by several authors (see [1–3, 5, 9, 18, 25, 28]). In the case $n=5$, Seidel [28] and Evans [9] proved that, in the monotone case, this group is homotopy equivalent to the group of orientation-preserving diffeomorphisms of S^2 preserving five points. Recently, Li, Li, and Wu in [18] completely determined the group of connected components of $\mathrm{Symp}_h(\mathbb{CP}^2\# 5\overline{\mathbb{CP}}^2,\omega)$, called the Torelli symplectic mapping class group, as well as the rank of its fundamental group, for any given symplectic form ω. In order to explain their results, which are of interest to us, we first recall the definition of reduced forms, and postpone further details to Section 2.3.

For $\mathbb{X}_n=\mathbb{CP}^2\# n\overline{\mathbb{CP}}^2$, let $\{L,V_1,\dots,V_n\}$ be a standard basis for $H_2(\mathbb{X}_n;\mathbb{Z})$, where L is the class representing a line, and the V_i are the exceptional classes.

Definition 1.1 Consider $\mathbb{X}_n$ with the standard basis $\{L,V_1,\dots,V_n\}$ of $H_2(\mathbb{X}_n;\mathbb{Z})$. Given a symplectic form ω such that each class $L,V_1,\dots,V_n$ has ω-area $\nu,\delta_1,\dots,\delta_n$, then ω is called *reduced* if

$$\nu>\delta_1\ge\cdots\ge\delta_n>0\quad\text{and}\quad\nu\ge\delta_1+\delta_2+\delta_3. \tag{1.1}$$

We recall in Section 2.3 why any symplectic form on $\mathbb{X}_n$ is diffeomorphic to a reduced one. Note that diffeomorphic symplectic forms yield homeomorphic symplectomorphism groups. Therefore, it suffices to understand the symplectomorphism group $\mathrm{Symp}(\mathbb{X}_n,\omega)$ for any reduced form ω. In this section, we also recall that $(\mathbb{X}_n,\omega)$ can be naturally identified with $(n-1)$-point blowups of the manifold

$(S^2 \times S^2, \mu\sigma \oplus \sigma)$, denoted by $M_{\mu,c_1,\dots,c_{n-1}}$, where σ denotes the standard symplectic form on S^2 that gives area 1 to the sphere, $\mu \geq 1$, and $c_1, \dots, c_{n-1}$ denote the capacities of the blowups.

If $n \leq 3$, it is well known that the group $\mathrm{Symp}_h(M_{\mu,c_1,\dots,c_n})$ is connected (see, for example, [17]) and it follows from [3, 5, 25] that the fundamental group of $\mathrm{Symp}_h(M_{\mu,c_1,\dots,c_n})$ is always generated by Hamiltonian circle actions. More precisely, in these cases, the full rational homotopy type of $\mathrm{Symp}_h(M_{\mu,c_1,\dots,c_n})$, with $n \leq 3$, is generated by loops in the fundamental group, represented by circle actions, via Samelson products. On the other hand, it was shown by Li and Li in [16] that if $n \leq 3$, then $\pi_1(\mathrm{Symp}_h(M_{\mu,c_1,\dots,c_n}))$ is a free abelian group.

In [18], the authors show that, in addition to the monotone case, there is a one-dimensional family of symplectic manifolds M_{μ,c_1,c_2,c_3,c_4} for which the Torelli symplectic mapping class group $\pi_0(\mathrm{Symp}_h(M_{\mu,c_1,c_2,c_3,c_4}))$ is isomorphic to $\pi_0(\mathrm{Diff}^+(S^2,4))$, where $\mathrm{Diff}^+(S^2,4)$ is the group of orientation-preserving diffeomorphisms of S^2 preserving four points. This family is defined by the values $\mu > 1$ and $c_i = 1/2$ for all $i \in \{1,2,3,4\}$. From now on, we use the notation $M_{\mu,c_i=1/2}$ to denote this family of symplectic manifolds. For all the remaining symplectic forms, the group $\pi_0(\mathrm{Symp}_h(M_{\mu,c_1,c_2,c_3,c_4}))$ is trivial. Moreover, in [18, Section 5.3], the authors show that $\pi_1(\mathrm{Symp}_h(M_{\mu,c_i=1/2})) = \mathbb{Z}^5$, and hence the fundamental group is a free abelian group.

In this note, we study generators of the fundamental group of $\mathrm{Symp}_h(M_{\mu,c_i=1/2})$. Our main result is the following theorem that gives a negative answer to the first part of Question 1.1.

Theorem 1.3 *If $1 < \mu \leq \frac{3}{2}$, then the set of all Hamiltonian circle actions generates a proper subgroup of rank 4 in the fundamental group of $\mathrm{Symp}_h(M_{\mu,c_i=1/2})$. Moreover, if $\mu > \frac{3}{2}$, then $\pi_1(\mathrm{Symp}_h(M_{\mu,c_i=1/2})) \otimes \mathbb{Q}$ is generated by Hamiltonian circle actions.*

To the best of our knowledge, this is the first example of symplectic rational surface where the fundamental group of $\mathrm{Symp}(\mathbb{X}_n, \omega)$ is not generated by circle actions. In Section 5, we discuss the existence of more symplectic forms ω in $\mathbb{X}_5$ for which a similar phenomenon may occur.

Remark 1.4 Although there is a generator of $\pi_1(\mathrm{Symp}_h(M_{\mu,c_i=1/2})) \otimes \mathbb{Q}$ which cannot be represented by a Hamiltonian circle action when $1 < \mu \leq \frac{3}{2}$, one can find its quantum homology representative (see Proposition 4.12).

Our techniques allows us to completely describe the elements of $\pi_1(\mathrm{Symp}_h(M_{\mu,c_i=1/2}))$ that are represented by Hamiltonian circle actions, answering the second part of Question 1.1 as well. In particular, we obtain the following result.

Theorem 1.5 *For any value of $\mu > 1$, there exist infinitely many homotopy classes in the fundamental group $\pi_1(\mathrm{Symp}_h(M_{\mu,c_i=1/2}))$ that cannot be represented by Hamiltonian circle actions.*

As a final remark, it seems very likely that Theorem 1.3 holds not only rationally but also in the integer case, that is, that the fundamental group $\pi_1(\mathrm{Symp}(M_{\mu,c_i=1/2}))$ is generated by Hamiltonian circle actions whenever $\mu > \frac{3}{2}$. Although we are not able to prove this stronger claim, we note that our quantum homology calculations imply the existence of five circle actions representing homotopy classes in $\pi_1(\mathrm{Symp}(M_{\mu,c_i=1/2}))$ that can be shown to be not only linearly independent but also primitive.

1.1 Organization of the paper

In Section 2, we review the main tools we need to prove the theorems above, namely Karshon's classification of Hamiltonian circle actions, Delzant's classification of toric manifolds, and the definitions of the quantum homology ring of a symplectic manifold and of the Seidel morphism. We also recall the results of [18] regarding π_0 and π_1 of the symplectomorphism group $\mathrm{Symp}_h(M_{\mu,c_1,c_2,c_3,c_4})$ relevant to our work. In Section 3, we give a presentation of the quantum homology ring $QH_*(M_{\mu,c_1,c_2,c_3,c_4})$, that follows from applying the formulas for the quantum product on a rational surface obtained by Crauder and Miranda in [7]. We dedicate Section 4 to obtaining our main results: we choose a tentative set of five generators of the rational fundamental group and prove, using the Seidel morphism, that these elements are linearly independent. We conclude this section giving a classification of all Hamiltonian circle actions on $M_{\mu,c_i=1/2}$, which allows us to determine which homotopy class of loops can be represented by such an action.

Finally, in the last section, we propose some further questions that arose naturally on the course of this work. Appendix A contains computations on the quantum ring, whereas Appendix B is devoted to the proof of an auxiliary relation between elements in $\pi_1(\mathrm{Symp}_h(M_{\mu,c_1,c_2,c_3,c_4}))$.

2 Background

2.1 Hamiltonian circle actions, decorated graphs, and Delzant polygons

In the forthcoming sections, we will study loops in the fundamental group of $\mathrm{Symp}_h(M_{\mu,c_1,c_2,c_3,c_4})$. Since these loops will appear as Hamiltonian circle actions, we will make extensive use of Karshon's classification of Hamiltonian circle actions and Delzant's classification of toric actions on symplectic manifolds. For convenience, we give a quick overview on how these classifications work.

Karshon's classification [10] yields a bijection between certain *decorated graphs* and 4-tuples $(M^4, \omega, \rho, \Phi)$ consisting of a symplectic 4-manifold (M^4, ω), and an effective Hamiltonian circle action ρ with a given moment map $\Phi : M \to \mathbb{R}$. Given such a tuple $(M^4, \omega, \rho, \Phi)$, the associated decorated graph is constructed as follows. Each component C of the fixed point set is either a single point or a symplectic surface, and fixed points on which the moment map is not extremal are isolated. For each such component C, there is a vertex $\langle C\rangle$, labeled by the real number $\Phi(C)$. A vertex that corresponds to a fixed symplectic surface is said to be "fat" and is given two more labels: the area label $\frac{1}{2\pi}\int_C \omega$, and the genus g of the surface. A $\mathbb{Z}_k$-*sphere* is a gradient sphere in M on which S^1 acts with isotropy $\mathbb{Z}_k$, $k \geq 2$. For each $\mathbb{Z}_k$-sphere containing

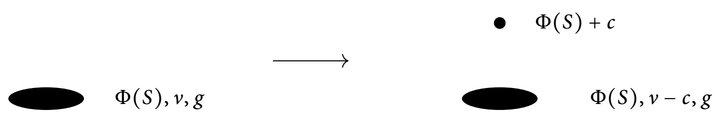

Figure 1: Blowing up at a point inside an invariant surface at the minimum value of Φ.

two fixed points p and q, the graph has an edge connecting the vertices $\langle p \rangle$ and $\langle q \rangle$ labeled by the integer k.

Labeled graphs associated with effective Hamiltonian circle actions are characterized by the following properties. If we order the vertices according to their moment map labels, then:

- there are exactly two extremal vertices;
- fat vertices are extremal, and if the graph contains two fat vertices, then their genus label must coincide;
- the area label of any fat vertex must be strictly positive;
- a vertex is connected to no more than two edges, and no edge is connected to a fat vertex;
- the moment map labels must be strictly monotone along each chain of edges;
- if $e_1, \dots, e_\ell$ is a chain of edges, and if $k_1, \dots, k_\ell$ are the orders of their stabilizers, then $\gcd(k_i, k_{i+1}) = 1$ for $i = 1, \dots \ell - 1$, and $(k_{i-1} + k_{i+1})/k_i$ is an integer for $i = 2, \dots, \ell - 1$.

We call such graphs *admissible*.

Theorem 2.1 (Karshon [10]) *Each* 4*-tuple* $(M^4, \omega, \rho, \Phi)$ *corresponds to a unique admissible labeled graph. Conversely, each admissible labeled graph corresponds to a* 4*-tuple* $(M^4, \omega, \rho, \Phi)$ *that is unique up to* S^1*-equivariant symplectomorphisms preserving the moment map.*

Furthermore, it can be shown that each Hamiltonian action on a four-dimensional manifold can be obtained from a circle action on a symplectic ruled surface by performing a sequence of S^1-equivariant symplectic blowups. At the graph level, equivariant symplectic blowups correspond to the simple transformations pictured in Figures 1 and 2. Together with Lalonde–McDuff–Li–Liu's uniqueness theorem [14, 19] stating that any two cohomologous symplectic forms on blowups of ruled surfaces are diffeomorphic, this gives an effective algorithm to enumerate all effective circle actions on any given 4-manifold.

Since we are mainly interested in the continuous map $\rho : S^1 \to \mathrm{Ham}(M, \omega)$, we do not need to keep track of the moment map associated with a Hamiltonian circle action. As any two moment maps only differ by a constant, we can either consider graphs only up to a uniform translation of their moment map labels, or normalize the moment map by setting $\min_{x \in M} \Phi(x) = 0$. Finally, note that the reparameterization of the circle $t \mapsto -t$ corresponds to changing the signs of the moment map labels.

There is an analogous classification of Hamiltonian toric actions that we now briefly describe in the special case of 4-manifolds. Given a 4-tuple $(M^4, \omega, \rho, \Phi)$ consisting

https://doi.org/10.4153/S0008414X22000323 Published online by Cambridge University Press

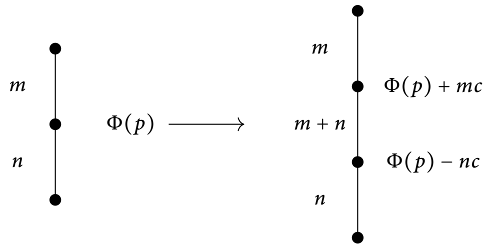

Figure 2: Blowing up at an interior fixed point.

of a symplectic 4-manifold (M,ω), an effective Hamiltonian toric action $\rho : T^2 \to \mathrm{Ham}(M,\omega)$, and a moment map $\Phi : M \to \mathfrak{t}^* \simeq \mathbb{R}^2$, the image $\Phi(M)$ is always a *Delzant polygon*, that is, a polygon satisfying the following three properties:

- simplicity, i.e., there are two edges meeting each vertex;
- rationality, i.e., the edges meeting at the vertex p are rational in the sense that each edge is of the form $p + tu_i$, $t \in [0,\ell_i]$, where $\ell_i \in \mathbb{R}$ and $u_i \in \mathbb{Z}^2$;
- smoothness, i.e., for each vertex, the corresponding u_1, u_2 can be chosen to be a $\mathbb{Z}$-basis of $\mathbb{Z}^2$.

Moreover, the preimage in the manifold of a vertex of the polygon $\Phi(M)$ is a fixed point for the torus action, whereas the preimage of an edge is an invariant 2-sphere. The preimage of the interior of the polygon consists of free torus orbits. These facts are explained in [8].

Delzant's classification [8] states that equivalence classes of 4-tuple (M^4,ω,ρ,Φ) up to equivariant symplectomorphisms that preserve the moment maps are classified by Delzant polygons in $\mathbb{R}^2$. If we disregard the moment map and only consider an effective toric action as an injective homomorphism $\rho : \mathbb{T}^2 \to \mathrm{Ham}(M,\omega)$, it is natural to declare two actions as equivalent if they only differ by a reparameterization of the torus or by a conjugation by an element of $\mathrm{Symp}(M,\omega)$. In this setting, the classification theorem yields a bijection

$$\{\text{Conjugacy classes of toric actions on 4-manifolds up to reparameterizations}\}$$
$$\updownarrow$$
$$\{\text{Delzant polygons in } \mathbb{R}^2 \text{ up to } \mathrm{AGL}(2;\mathbb{Z}) \text{ action}\}.$$

If we restrict the action to the subcircle $\{e\}\times S^1$, we get a compact four-dimensional S^1-space. The moment map for the S^1-action is the composition of the $\mathbb{T}^2$-moment map with the projection $\mathbb{R}^2 \to \mathbb{R}$ to the second coordinate. The fixed surfaces are the preimages, under the $\mathbb{T}^2$-moment map, of the horizontal edges of the Delzant polygon. Such a surface has genus zero, and its normalized symplectic area is equal to the length of the corresponding horizontal edge. The isolated fixed points are the preimages of those vertices of the polygon that do not lie on horizontal edges. The $\mathbb{Z}_k$-spheres, $k \geq 2$, are the preimages of edges with slope $\pm k/b$ in a reduced form, where b is relatively prime to k. With this information, we can construct the graph for the

S^1-space out of the Delzant polygon. This is explained by Karshon in [10, Section 2.2]. Note that, similarly, we can restrict the toric action to the subcircle $S^1 \times \{e\}$ in order to obtain another compact four-dimensional S^1-space. In this case, the moment map for the S^1-action is the composition of the $\mathbb{T}^2$-moment map with the projection $\mathbb{R}^2 \to \mathbb{R}$ to the first coordinate. This relation between polygons and decorated graphs will be particularly useful in the following subsections.

2.2 Quantum homology and Seidel morphism

Following [23], consider the (small) quantum homology ring $QH_*(M;\Pi) = H_*(M,\mathbb{Q}) \otimes_{\mathbb{Q}} \Pi$ with coefficients in the ring $\Pi := \Pi^{\mathrm{univ}}[q,q^{-1}]$ where the q is a polynomial variable of degree 2 and Π^{univ}, called the universal Novikov ring, is a generalized Laurent series ring in a variable t of degree 0:

$$\Pi^{\mathrm{univ}} := \left\{ \sum_{\kappa\in\mathbb{R}} r_\kappa t^\kappa \,\middle|\, r_\kappa \in \mathbb{Q},\ \#\{\kappa > c \mid r_\kappa \neq 0\} < \infty, \forall c \in \mathbb{R} \right\}. \tag{2.1}$$

The quantum homology $QH_*(M;\Pi)$ is $\mathbb{Z}$-graded so that $\deg(a\otimes q^d t^\kappa) = \deg(a) + 2d$ with $a \in H_*(M)$. The *quantum intersection product* $a * b \in QH_{i+j-\dim M}(M;\Pi)$, of classes $a \in H_i(M)$ and $b \in H_j(M)$, has the form

$$a * b = \sum_{B\in H_2^S(M;\mathbb{Z})} (a*b)_B \otimes q^{-c_1(B)} t^{-\omega(B)},$$

where $H_2^S(M;\mathbb{Z})$ is the image of $\pi_2(M)$ under the Hurewicz map. The homology class $(a*b)_B \in H_{i+j-\dim M+2c_1(B)}(M)$ is defined by the requirement that

$$(a*b)_B \cdot_M c = \mathrm{GW}^M_{B,3}(a,b,c) \qquad \text{for all } c \in H_*(M).$$

In this formula, $\mathrm{GW}^M_{B,3}(a,b,c) \in \mathbb{Q}$ denotes the Gromov–Witten invariant that counts the number of spheres in M in class B that meet cycles representing the classes $a, b, c \in H_*(M)$. The product $*$ is extended to $QH_*(M)$ by linearity over Π, and is associative (see [23, Proposition 11.1.9] for a proof of this fact). It also respects the $\mathbb{Z}$-grading and gives $QH_*(M)$ the structure of a graded commutative ring, with unit $[M]$.

The *Seidel morphism* is a homomorphism $\mathcal{S}$ from $\pi_1(\mathrm{Ham}(M,\omega))$ to the degree $2n$ multiplicative units $QH_{2n}(M)^\times$ of the small quantum homology, first introduced by Seidel in [27]. One way of thinking of it is to say that it “counts” pseudoholomorphic sections of the bundle $M_\Lambda \to S^2$ associated with the loop $\Lambda \subset \mathrm{Ham}(M,\omega)$ via the clutching construction (as in [24, Section 2]): let (M,ω) be a closed symplectic manifold and let $\Lambda = \{\Lambda_\theta\}$ be a loop in $\mathrm{Ham}(M,\omega)$ based on identity. Denote by M_Λ the total space of the fibration over S^2 with fiber M which consists of two trivial fibrations over 2-discs, glued along their boundary via Λ. Namely, we consider S^2 as the union of the two 2-discs D_0 and D_∞ such that D_0 is the closed unit disk centered at 0 in the Riemann sphere $S^2 = \mathbb{C}\cup\{\infty\}$ and D_∞ is another copy of this disk, embedded in $S^2 = \mathbb{C}\cup\{\infty\}$, via the orientation reversing map $r\,e^{i\theta} \mapsto r^{-1}\,e^{i\theta}$. The total space is

$$M_\Lambda = \big(M\times D_0\big)\bigsqcup\big(M\times D_\infty\big)/\sim \quad \text{with } (e^{2i\pi\theta}, \Lambda_\theta(x))_0 \sim (e^{2i\pi\theta}, x)_\infty.$$

This construction only depends on the homotopy class of Λ. Moreover, the family (parameterized by S^2) of symplectic forms of the fibers can be extended to give a

https://doi.org/10.4153/S0008414X22000323 Published online by Cambridge University Press

closed form, Ω, on M_Λ (see [29]). By adding to Ω the pullback of a suitable area form on the base, we get a nondegenerate form. More precisely, $\omega_{\Lambda,\kappa} = \Omega + \kappa \cdot \pi^*(\omega_0)$ is symplectic, where ω_0 is the standard symplectic form on S^2 (with area 1), π is the projection to the base of the fibration, and κ is a big enough constant to make $\omega_{\Lambda,\kappa}$ nondegenerate. (Once chosen, κ will be omitted from the notation.)

So we end up with the following Hamiltonian fibration:

$$(M,\omega) \hookrightarrow (M_\Lambda,\omega_\Lambda) \xrightarrow{\pi} (S^2,\omega_0).$$

In [24], McDuff and Tolman observed that, when Λ is a circle action (with associated moment map Φ_Λ), the clutching construction can be simplified since, then, M_Λ can be seen as the quotient of $M \times S^3$ by the diagonal action of S^1, $e^{2\pi i\theta} \cdot (x,(z_1,z_2)) = (\Lambda_\theta(x),(e^{2\pi i\theta} z_1, e^{2\pi i\theta} z_2))$. The symplectic form also has an alternative description in $M \times_{S^1} S^3$. Let $\alpha \in \Omega^1(S^3)$ be the standard contact form on S^3 such that $d\alpha = \chi^*(\omega_0)$ where $\chi : S^3 \to S^2$ is the Hopf map and ω_0 is the standard area form on S^2 with total area 1. For all $c \in \mathbb{R}$, $\omega + cd\alpha - d(\Phi_\Lambda\alpha)$ is a closed 2-form on $M \times S^3$ which descends through the projection, $p : M \times S^3 \to M \times_{S^1} S^3$, to a closed 2-form on M_Λ:

$$\omega_c = p(\omega + cd\alpha - d(\Phi_\Lambda\alpha)), \tag{2.2}$$

which extends Ω. Now, if $c > \max \Phi_\Lambda$, ω_c is nondegenerate and coincides with $\omega_{\Lambda,\kappa}$ for some big enough κ.

A quantum class lying in the image of $\mathcal{S}$ is called a *Seidel element*. In [24], McDuff and Tolman were able to calculate the leading term of Seidel's elements associated with Hamiltonian circle actions whose maximal fixed point component, $F_{\max}$, is semi-free, that is, the action is semi-free on some neighborhood of $F_{\max}$. Recall that a circle action is semi-free if the stabilizer of every point is trivial or the whole circle. Moreover, when the codimension of $F_{\max}$ is 2, their result immediately ensures that if there exists an invariant almost complex structure J on M so that (M,J) is Fano, i.e., so that there are no J-pseudoholomorphic spheres in M with nonpositive first Chern number, all the lower-order terms vanish. In the presence of J-pseudoholomorphic spheres with vanishing first Chern number, there is a priori no reason why arbitrarily large multiple coverings of such objects should not contribute to the Seidel elements. In fact, as explained in [4], when the almost complex manifold (M,J) is only numerically effective (NEF), i.e., $c_1(B) \geq 0$ for every class $B \in H_2(M)$ with a J-holomorphic sphere representative, and not Fano, then there are indeed infinitely many contributions to the Seidel elements. More precisely, it is shown in [4] that if M is a 4-toric manifold, then these quantum classes can still be expressed by explicit closed formulas. Moreover, these formulas only depend on the relative position of representatives of elements of $\pi_2(M)$ with vanishing first Chern number as edges of the moment polygon. In particular, they are directly readable from the polygon.

We now recall the precise results from [4] that we will use in the forthcoming sections. Consider a four-dimensional closed symplectic manifold (M,ω), endowed with a toric structure (ρ,Φ). Suppose that the associated Delzant polygon $P = \Phi(M)$ has $m \geq 4$ edges, and consider a Hamiltonian circle action Λ on (M,ω), with moment map Φ_Λ, such that Λ is a subcircle of the toric action $\rho : \mathbb{T}^2 \to \mathrm{Ham}(M,\omega)$.

https://doi.org/10.4153/S0008414X22000323 Published online by Cambridge University Press

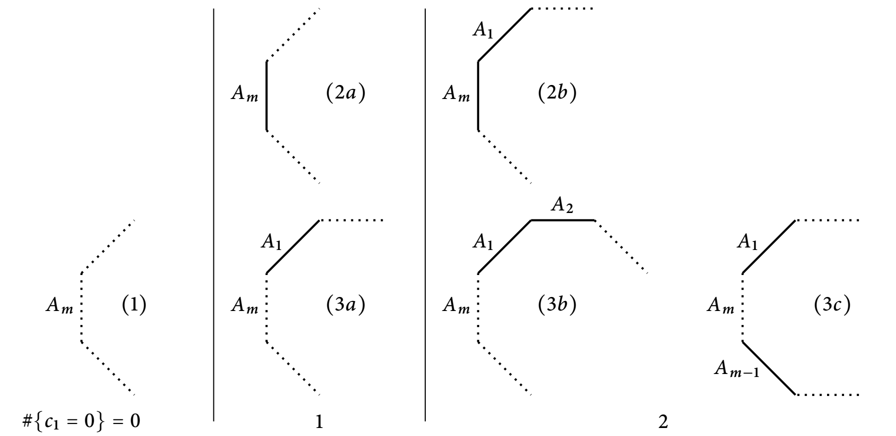

Figure 3: Cases appearing in Theorem 2.2.

We assume additionally that the fixed point component of Λ on which Φ_Λ is maximal is a 2-sphere, $F_{\max} \subset M$, whose momentum image is an edge D of P. We denote by $A \in H_2(M;\mathbb{Z})$ the homology class of $F_{\max}$ and by $\Phi_{\max} = \Phi_\Lambda(F_{\max})$.

In this case, McDuff–Tolman's result [24, Theorem 1.10] ensures that the Seidel element associated with Λ is

$$\mathcal{S}(\Lambda) = A \otimes qt^{\Phi_{\max}} + \sum_{B \in H_2^S(M;\mathbb{Z})^{>0}} a_B \otimes q^{1-c_1(B)} t^{\Phi_{\max} - \omega(B)}, \tag{2.3}$$

where $H_2^S(M;\mathbb{Z})^{>0}$ consists of the spherical classes of positive symplectic area, that is, $\omega(B) > 0$ and $a_B \in H_*(M;\mathbb{Z})$ denotes the contribution of B. As mentioned above, when (M, J) is Fano for some S^1-invariant ω-compatible almost complex structure J, then all the lower-order terms vanish and we end up with $\mathcal{S}(\Lambda) = A \otimes qt^{\Phi_{\max}}$.

In the non-Fano case, one has to be careful about the number and relative position of edges, in the vicinity of D, corresponding to spheres in M with vanishing first Chern number. We denote the number of such edges by $\#\{c_1 = 0\}$. We denote the edges and the corresponding homology classes in M in a cyclic way, that is, D, which, we denote by D_m below, has neighboring edges D_{m-1} on one side and $D_{m+1} = D_1$ on the other, and they, respectively, induce classes A_m, A_{m-1}, and $A_{m+1} = A_1$ in $H_2(M;\mathbb{Z})$.

Figure 3 shows the relevant parts of the different polygons we need to consider. Dotted lines represent edges with positive first Chern number, and we indicate near each edge with nontrivial contribution the homology class of the corresponding sphere in M. For example, in Case *(3c)*, only three homology classes contribute: A_{m-1}, A_m, and A_1; A_{m-1} and A_1 have vanishing first Chern number while $c_1(A_m) \neq 0$.

Now, the following theorem gives the explicit expression of the Seidel element associated with Λ when $\#\{c_1 = 0\} \leq 2$.

Theorem 2.2 [4, Theorem 4.5] *Let (M, ω) be a four-dimensional closed symplectic manifold, endowed with a toric structure. With the notation described above, assume*

https://doi.org/10.4153/S0008414X22000323 Published online by Cambridge University Press

that the Delzant polygon P has $m \geq 4$ edges, and that the fixed point component of the Hamiltonian action Λ on which Φ_Λ is maximal is a 2-sphere, $F_{\max} \subset M$. Additionally, assume that (M,J) is NEF, for some S^1-invariant ω-compatible almost complex structure J. Then, in the cases described by Figure 3, the Seidel element associated with Λ is:

(1) $\mathcal{S}(\Lambda) = A_m \otimes q t^{\Phi_{\max}}$;

(2a) $\mathcal{S}(\Lambda) = A_m \otimes q \dfrac{t^{\Phi_{\max}}}{1-t^{-\omega(A_m)}}$;

(2b) $\mathcal{S}(\Lambda) = \left(A_m \otimes q \dfrac{t^{\Phi_{\max}}}{1-t^{-\omega(A_m)}} - A_1 \otimes q \dfrac{t^{\Phi_{\max}-\omega(A_1)}}{1-t^{-\omega(A_1)}}\right)\dfrac{1}{1-t^{-\omega(A_m)-\omega(A_1)}}$;

(3a) $\mathcal{S}(\Lambda) = A_m \otimes q t^{\Phi_{\max}} - A_1 \otimes q \dfrac{t^{\Phi_{\max}-\omega(A_1)}}{1-t^{-\omega(A_1)}}$;

(3b) $$\mathcal{S}(\Lambda) = A_m \otimes q t^{\Phi_{\max}} - A_1 \otimes q \frac{t^{\Phi_{\max}-\omega(A_1)}}{1-t^{-\omega(A_1)}} - \left(A_1 \otimes q \frac{t^{\Phi_{\max}}}{1-t^{-\omega(A_1)}} - A_2 \otimes q \frac{t^{\Phi_{\max}-\omega(A_2)}}{1-t^{-\omega(A_2)}}\right)\frac{t^{-\omega(A_1)-\omega(A_2)}}{1-t^{-\omega(A_1)-\omega(A_2)}};$$

(3c) $\mathcal{S}(\Lambda) = A_m \otimes q t^{\Phi_{\max}} - A_{m-1} \otimes q \dfrac{t^{\Phi_{\max}-\omega(A_{m-1})}}{1-t^{-\omega(A_{m-1})}} - A_1 \otimes q \dfrac{t^{\Phi_{\max}-\omega(A_1)}}{1-t^{-\omega(A_1)}}$.

2.3 The fundamental group of Symp$(M_{\mu,c_1,c_2,c_3,c_4})$

In this section, we recall the main results obtained by Li et al. [18] on the Torelli symplectic mapping class group and on the rank of the fundamental group of the group $\mathrm{Symp}_h(M_{\mu,c_1,c_2,c_3,c_4})$ of symplectomorphisms that act trivially on homology, for any given symplectic form.

First, note that diffeomorphic symplectic forms define symplectomorphism groups that are homeomorphic, and that symplectomorphism groups are invariant under rescalings of symplectic forms. Consequently, we can restrict ourselves to symplectic forms belonging to a fundamental domain for the action of $\mathrm{Diff} \times \mathbb{R}_*$ on the space Ω_+ of orientation-compatible symplectic forms defined on the n-fold blowup $\mathbb{X}_n$. The cohomology class of a reduced class ω (see Definition 1.1 in the Introduction) is $\nu L - \delta_1 V_1 - \cdots - \delta_n V_n$. Let $\mathcal{J}_\omega$ be the space of compatible almost complex structures on $\mathbb{X}_n$. For any $J \in \mathcal{J}_\omega$ on $\mathbb{X}_n$, the first Chern class $c_1 := c_1(TM) \in H^2(\mathbb{X}_n;\mathbb{Z})$ is the Poincaré dual to $K := 3L - \sum_i V_i$. Let $\mathcal{K}$ be the symplectic cone of $\mathbb{X}_n$, that is,

$$\mathcal{K} = \{A \in H^2(\mathbb{X}_n;\mathbb{Z}) \mid A = [\omega] \text{ for some symplectic form } \omega \in \Omega_+\}.$$

Now, if C stands for the Poincaré dual of the symplectic cone of $\mathbb{X}_n$, then by *uniqueness of symplectic blowups* proved by McDuff in [22], the diffeomorphism class of the form ω only depends on its cohomology class. Therefore, it is enough to describe a fundamental domain of the action of $\mathrm{Diff} \times \mathbb{R}_*$ on C. Moreover, the canonical class K is unique up to orientation-preserving diffeomorphisms [20], so it suffices to describe the action of the diffeomorphisms fixing K, Diff_K, on

$$C_K = \{A \in H_2(\mathbb{X}_n;\mathbb{R}) \ :\ A = PD[\omega] \text{ for some } \omega \in \Omega_K\},$$

where Ω_K is the set of orientation-compatible symplectic forms with K as the symplectic canonical class. By the results in [20], the set of reduced classes is a fundamental domain of $C_K(\mathbb{X}_n)$ under the action of Diff_K. A proof of this result is also given in [11, Theorem 1.4]. We now consider the following change of basis in $H_2(\mathbb{X}_n;\mathbb{Z})$. Consider the symplectic manifold $(S^2 \times S^2, \mu\sigma \oplus \sigma)$ where the homology class of the base $B \in H_2(S^2 \times S^2)$ represented by $S^2 \times \{pt\}$ has area μ, and the homology class of the fiber $F \in H_2(S^2 \times S^2)$ represented by $\{pt\} \times S^2$ has area 1. Recall that $M_{\mu,c_1,\dots,c_{n-1}} = (S^2 \times S^2 \# (n-1)\overline{\mathbb{CP}}^2, \omega_{\mu,c_1,\dots,c_{n-1}})$ is obtained from $(S^2 \times S^2, \mu\sigma \oplus \sigma)$, by performing $n-1$ successive blowups of capacities $c_1, \dots, c_{n-1}$. This can be naturally identified with $(\mathbb{X}_n, \omega)$. One easy way to understand the equivalence is as follows: let $\{B, F, E_1, \dots, E_{n-1}\}$ be the basis for $H_2(M_{\mu,c_1,\dots,c_{n-1}};\mathbb{Z})$ where the E_i represent the exceptional spheres arising from the blowups. We identify L with $B + F - E_1$, V_1 with $B - E_1$, V_2 with $F - E_1$, and V_i with E_{i-1}, with $3 \le i \le n$. Then the *uniqueness of symplectic blowups* due to McDuff (see [22, Corollary 1.3]) implies that the symplectomorphism type of a symplectic blowup of a rational ruled manifold along an embedded ball of capacity $c \in (0,1)$ depends only on the capacity c and not on the particular embedding used in obtaining the blowup. Using this result and after rescaling, we conclude that, for parameters satisfying the relations

$$\mu = \frac{\nu - \delta_2}{\nu - \delta_1}, \quad c_1 = \frac{\nu - \delta_1 - \delta_2}{\nu - \delta_1}, \quad \text{and} \quad c_i = \frac{\delta_{i+1}}{\nu - \delta_1}, \quad 2 \le i \le n-1, \tag{2.4}$$

there exists a symplectomorphism between two symplectic manifolds encoded by these parameters such that

$$\nu L - \delta_1 V_1 - \cdots - \delta_n V_n = \mu B + F - c_1 E_1 - \cdots - c_{n-1} E_{n-1}.$$

Summarizing the above discussion, we showed that

Lemma 2.3 *Every symplectic form on $S^2 \times S^2 \# (n-1)\overline{\mathbb{CP}}^2$ is, after rescaling, diffeomorphic to a form Poincaré dual to $\mu B + F - c_1 E_1 - \cdots - c_{n-1} E_{n-1}$ with*

$$0 < c_{n-1} \le \cdots \le c_1 \le 1 \le \mu \quad \text{and} \quad c_i + c_j \le 1.$$

Recall (see [16]) that the normalized reduced symplectic cone is defined as the space of reduced symplectic classes having area 1 on L, the line class. Note that cohomologous symplectic forms on a rational or ruled surface are diffeomorphic (cf. [15, 20]). We represent such a class by $(1|\delta_1, \dots, \delta_n)$, or $(\delta_1, \dots, \delta_n) \in \mathbb{R}^n$. For $3 \le n \le 8$, such a cone is a n-simplex with one facet removed, where the monotone class is one of the vertices, namely $M_n = (\frac{1}{3}, \dots, \frac{1}{3})$. We are interested in the case when the manifold is $\mathbb{X}_5$ where the normalized reduced cone is convexly generated by five half-closed intervals $\{MO, MA, MB, MC, MD\}$, with vertices $M = (\frac{1}{3}, \frac{1}{3}, \frac{1}{3}, \frac{1}{3}, \frac{1}{3})$, which corresponds to the monotone case, $O = (0,0,0,0,0)$, $A = (1,0,0,0,0)$, $B = (\frac{1}{2}, \frac{1}{2}, 0, 0, 0)$, $C = (\frac{1}{3}, \frac{1}{3}, \frac{1}{3}, 0, 0)$, and $D = (\frac{1}{3}, \frac{1}{3}, \frac{1}{3}, \frac{1}{3}, 0)$ (for more details, see [16]).

Let N_ω be the number of symplectic-2 spheres classes. Then Li, Li, and Wu proved the following.

Theorem 2.4 [18, Theorem 1.2] *Consider $\mathbb{X}_5$ with any symplectic form ω. Then the rank of the fundamental group of* $\mathrm{Symp}_h(\mathbb{X}_5, \omega)$ *satisfies*

$$\mathrm{rank}(\pi_1(\mathrm{Symp}_h(\mathbb{X}_5, \omega))) = N_\omega - 5 + \mathrm{rank}(\pi_0(\mathrm{Symp}_h(\mathbb{X}_5, \omega))),$$

where the rank of $\pi_0(\mathrm{Symp}_h(\mathbb{X}_5, \omega))$ means the rank of its abelianization.

Moreover, along the edge MA, when $\nu=1, \delta_1>\delta_2=\delta_3=\delta_4=\delta_5$, and $\delta_1+\delta_2+\delta_3=1$, or equivalently, when $\mu>1$ and $c_1=c_2=c_3=c_4=1/2$, it follows from [18, Lemma 5.10] and its proof (in particular from sequence (37)) that $\pi_1(\mathrm{Symp}_h(\mathbb{X}_5,\omega))=\mathbb{Z}_5$. This is the case we will study in detail in the forthcoming sections. In particular, we will show that a generating set of the fundamental group of $\mathrm{Symp}_h(\mathbb{X}_5,\omega)$ can be realized by Hamiltonian circle actions except in some particular interval of values of μ.

3 Quantum homology of M_{μ,c_1,c_2,c_3,c_4}

In [7], Crauder and Miranda compute the quantum cohomology of a general rational surface, which includes the case of the blown-up manifold $\mathbb{CP}^2\#5\overline{\mathbb{CP}^2}$. Using Poincaré duality, this allows us to construct a presentation for the quantum homology ring $QH_*(M_{\mu,c_1,c_2,c_3,c_4})$, so that we can then compare different Seidel elements. The relations

$$\begin{cases} L=B+F-E_1,\\ V_1=B-E_1,\\ V_2=F-E-1,\\ V_i=E_{i-1}, \text{ for } 2\le i\le n,\end{cases}$$

give an explicit way of translating information in terms of the classes $\{L,V_1,\dots,V_n\}$ to one in terms of $\{B,F,E_1,\dots,E_{n-1}\}$.

An explicit formula for the quantum product in terms of the classes L, V_i is given in Proposition 5.3 of [7]. The coefficients that appear in these can be computed with the help of the tables in Section 4 of [7], giving us a closed formula for the products we are interested in. As an example, the product of two classes, different from the class of a single point $p\in H_0(\mathbb{X}_5,\mathbb{Z})$, in $\mathbb{CP}^2\#5\overline{\mathbb{CP}^2}$, is given by

$$\begin{aligned}(dL-\sum_i m_iV_i)*(d'L-\sum_i m_i'V_i) &= \left(dd'-\sum_i m_im_i'\right)pt^{[p]}+\sum_k m_km_k'V_kt^{[V_k]}\\ &+\sum_{j,k}(d-m_j-m_k)(d'-m_j'-m_k')(L-V_j-V_k)t^{[L-V_j-V_k]}\\ &+\left(2d-\sum_i m_i\right)\left(2d'-\sum_i m_i'\right)(2L-V_1-V_2-V_3-V_4-V_5)t^{[2L-V_1-V_2-V_3-V_4-V_5]}\\ &+\sum_j(d-m_j)(d'-m_j')Xt^{[L-V_j]}\\ &+\sum_{j,k,l,n}(2d-m_j-m_k-m_l-m_n)(2d'-m_j'-m_k'-m_l'-m_n')Xt^{[2L-V_j-V_k-V_l-V_n]},\end{aligned}$$

where i,j,k,l,n always represent distinct indices, $X\in H_4(\mathbb{X}_5,\mathbb{Z})$ is the class of the manifold, $d\in\mathbb{Z}_{>0}$, $m_i,m_j'\in\mathbb{Z}_{\ge0}$, and $t^{[A]}$ means t to the power of the negative symplectic area of the corresponding class A (in the symplectic viewpoint).

The next proposition gives a description of the ring $QH_*(M_{\mu,c_i=1/2})$. For the sake of simpler notation, let

$$b_{ij} = (B - E_i - E_j) \otimes q\,\frac{t^{\frac{1}{2}}}{1 - t^{1-\mu}}, \quad f_{ij} = (F - E_i - E_j) \otimes q\,\frac{t^{\frac{1}{2}}}{1 - t^{1-\mu}}, \quad \text{and}$$

$$e_i = E_i \otimes q\,\frac{t^{\frac{1}{2}}}{1 - t^{1-\mu}},$$

and, as before, let distinct letters in the indices correspond to distinct elements. Its proof is just computing the quantum products by the formula above and then translating them to a formula in terms of $\{B, F, E_1, \dots, E_4\}$. It follows from [7, Proposition 5.3] that we have the presentation for $QH_*(M_{\mu,c_i=1/2})$ given below.

Proposition 3.1 *With the notation above, when $\mu > 1$, as a Π^{univ}-algebra, we have*

$$QH_*(M_{\mu,c_i=1/2}) \simeq \Pi^{\text{univ}}[f_{ij},\ b_{ij},\ e_i]/I_{\mu,c_i=1/2},$$

where Π^{univ} is the universal Novikov ring and $I_{\mu,c_i=1/2}$ is the ideal generated by

(1) $b_{ij}b_{k\ell} = 1$;

(2) $b_{ij}b_{ik} = b_{ij}f_{ij} + f_{j\ell} + 1$;

(3) $b_{ij}^2 = 2b_{ij}f_{ij} + f_{ij} + f_{k\ell} + 1$;

(4) $f_{ik}(b_{ij} + 1) = 0$;

(5) $b_{ij}\left(f_{ij} + e_i + \dfrac{t^{1-\mu}}{1 - t^{1-\mu}}\right) = e_j + \dfrac{t^{1-\mu}}{1 - t^{1-\mu}}$;

(6) $b_{ij}\left(e_k + \dfrac{t^{1-\mu}}{1 - t^{1-\mu}}\right) = f_{k\ell} + e_\ell + \dfrac{t^{1-\mu}}{1 - t^{1-\mu}}$;

(7) $f_{ij}f_{k\ell} = 0$;

(8) $f_{ij}f_{ik} = f_{ij}(b_{ij} + 1)$;

(9) $f_{ij}^2 = 2f_{ij}(b_{ij} + 1)$;

(10) $(f_{ij} + f_{k\ell})(b_{ij} + 1) = 0$;

(11) $f_{ij}\left(b_{ij} + e_i + \dfrac{1}{1 - t^{1-\mu}}\right) = 0$;

(12) $f_{ij}\left(e_k + \dfrac{t^{1-\mu}}{1 - t^{1-\mu}}\right) = 0$;

(13) $e_ie_j = (2b_{ij} + 2f_{k\ell} + e_k + e_\ell)\dfrac{t^{1-\mu}}{1 - t^{1-\mu}} + \dfrac{2t^{1-\mu} + t^{2-2\mu}}{(1 - t^{1-\mu})^2}$;

(14) $e_i^2 = b_{ij}f_{ij} + \dfrac{f_{ij}}{1 - t^{1-\mu}} + (2b_{ij} + f_{k\ell} + 2e_j)\dfrac{t^{1-\mu}}{1 - t^{1-\mu}} + \dfrac{2t^{1-\mu} + t^{2-2\mu}}{(1 - t^{1-\mu})^2}$. ∎

Remark 3.2 Of course, our description does not give a minimal set of generators nor is that the intention of Proposition 3.1. The generators were picked with the intent of simplifying the computations of the Seidel morphism and they also give some simple insight into the ring structure: for instance, relation $f_{ij}f_{k\ell} = 0$ implies that there are zero divisors.

4 Generators of $\pi_1(\mathbf{Symp}(M_{\mu,c_1,c_2,c_3,c_4}))$

4.1 Hamiltonian circle actions in M_{μ,c_1,c_2,c_3,c_4}

In this section, we list all equivalence classes of Hamiltonian circle actions on symplectic manifolds whose symplectic cohomology class belongs to the edge MA of

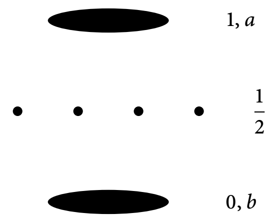

Figure 4: Graphs representing Hamiltonian circle actions on symplectic manifolds belonging to the ray MA.

the reduced symplectic cone. Recall that, along this edge, we have $\mu > 1$ and $c_1 = c_2 = c_3 = c_4 = 1/2$. Recall also that Karshon's classification [10, Section 6.2] implies that every compact four-dimensional Hamiltonian S^1-space can be obtained from a *minimal space*, which can be $\mathbb{CP}^2$, a Hirzebruch surface, or an irrational ruled manifold (see [10, Section 6.3]), by a sequence of equivariant symplectic blowups at fixed points. It follows that the only possible Hamiltonian circle actions on the symplectic manifolds belonging to the edge MA are the ones corresponding to the labeled graphs of Figure 4, where the values of a and b represent the symplectic area of the invariant spheres and depend on which sphere we perform the blowup. In our figures, we omit the genus label since, in our case, the invariant surfaces are always embedded spheres. Moreover, since the symplectic area of the spheres is positive, i.e., $a, b > 0$, and $c_1 = c_2 = c_3 = c_4 = 1/2$, then we can only have $a + b = 2\mu - 2$.

4.2 Circle actions and homotopy classes of loops

A labeled graph only determines a circle action up to symplectomorphisms. Equivalently, a labeled graph defines a conjugacy class of circles in $\mathrm{Symp}(M,\omega)$. Consequently, any such graph defines an element of

$$\pi_1(\mathrm{Symp}(M,\omega))\,/\,\mathrm{Symp}(M,\omega) \simeq \pi_1(\mathrm{Symp}(M,\omega))\,/\pi_0(\mathrm{Symp}(M,\omega)),$$

where the action is by conjugation. The analysis of this action is done in two stages.

For any symplectic manifold (M,ω) belonging to the ray MA, the action of $\mathrm{Symp}(M,\omega)$ on homology induces a short exact sequence

$$1 \to \mathrm{Symp}_h(M,\omega) \to \mathrm{Symp}(M,\omega) \xrightarrow{f} \mathrm{Aut}_{c_1,[\omega]}(H_2(M,\mathbb{Z})) \to 1,$$

where $\mathrm{Aut}_{c_1,[\omega]}(H_2(M,\mathbb{Z}))$ is the group of automorphisms of the lattice $H_2(M,\mathbb{Z})$ preserving the intersection form and the classes dual to $c_1(M,\omega)$ and $[\omega]$. The fact that the map f is onto follows from three results in [21] that we briefly recall. First,

https://doi.org/10.4153/S0008414X22000323 Published online by Cambridge University Press

by [21, Proposition 4.14], the group $\mathrm{Aut}_{c_1,[\omega]}(H_2(M,\mathbb{Z}))$ is generated by reflections about spherical homology classes A satisfying three conditions: $A \cdot A = -2$, $c_1(A) = 0$, and $\omega(A) = 0$. Such a class is called a $(K,[\omega])$-null spherical class, where K denotes the symplectic canonical class. Second, a symplectic Dehn twist along a Lagrangian sphere L induces the reflection $R([L])$ in homology. Finally, the result follows from Proposition 5.6 in [21] which proves existence of Lagrangian spheres representing $(K,[\omega])$-null spherical classes.

In our case, along MA, the automorphism group is isomorphic to the Weyl group D_4 given by the trivalent Dynkin diagram (see [18]). It is easy to see that it fixes the classes $2B + 2F - E_1 - E_2 - E_3 - E_4$ and F, whereas it acts transitively on the eight exceptional classes $E_1, \ldots, E_4, F - E_1, \ldots, F - E_4$. In particular, the only element of $\mathrm{Aut}_{c_1,[\omega]}$ that fixes the four exceptional classes E_i is the identity.

In order to keep track of the action of $\mathrm{Aut}_{c_1,[\omega]} \simeq \mathrm{Symp}(M,\omega)/\mathrm{Symp}_h(M,\omega)$ on Hamiltonian circle actions, we consider *extended graphs* as defined in [10, Section 5, p. 33] decorated with *homology labels*. Starting with the standard labelled graph of Figure 4, we add extra (dotted) edges that represent free invariant spheres connecting each interior fixed point to extrema of the moment map. Each such sphere is the closure of a free $\mathbb{C}^*$-orbit, where the $\mathbb{C}^*$ action is defined from the choice of a generic S^1-invariant almost-complex structure. Since the action of $\mathrm{Symp}(M,\omega)$ preserves the genericity of almost-complex structures, an extended graph defines a configuration of invariant spheres that is well defined up to conjugation. We then label the edges of the extended graph with homology classes according to the sequence of blowups that is used to construct the Hamiltonian S^1-manifold. Geometrically, this amounts to labeling invariant spheres with their homology class following a specific sequence of equivariant blowups performed on $\left(S^2 \times S^2, \mu\sigma \otimes \sigma\right)$, starting with the two fixed surfaces labeled $B = [S^2 \times \mathrm{pt}]$ and $F = [\mathrm{pt} \times S^2]$. The possible extended labeled graphs are shown in Figures 5–7. By construction, the group $\mathrm{Symp}(M,\omega)$ acts on its corresponding extended labeled graph with kernel $\mathrm{Symp}_h(M,\omega)$. In our case, these extended labeled graphs classify Symp_h-equivalence classes of S^1-manifolds on the edge MA endowed with a given framing $\phi : H_2(M,\mathbb{Z}) \to \mathbb{Z}\langle B, F, E_1, E_2, E_3, E_4\rangle \simeq \mathbb{Z}^{1,5}$.

Recall from [18] that, for (M,ω) belonging to the edge MA, the symplectomorphism group $\mathrm{Symp}_h(M,\omega)$ is not connected. Indeed, $\pi_0(\mathrm{Symp}_h(M,\omega)) = \pi_0(\mathrm{Diff}^+(S^2,4)) \simeq P_4(S^2)/\mathbb{Z}_2$, where $P_4(S^2)$ is the pure braid group of four strings in S^2. Since an extended labeled graph only determines an element in $\pi_1(\mathrm{Symp}(M,\omega))/\pi_0(\mathrm{Symp}_h(M,\omega))$, we have to understand how $\pi_0(\mathrm{Symp}_h(M,\omega))$ acts on $\pi_1(\mathrm{Symp}(M,\omega))$. We postpone this analysis to Section 4.4.

4.3 Extended labeled graphs along the edge MA

We now describe a finite set of one-parameter families of extended labeled graphs, parameterized by μ, that correspond to symplectic manifolds belonging to the edge MA of the reduced symplectic cone. The number of elements in these families depends on the range of μ. As explained above, each such graph corresponds to a $\mathrm{Symp}_h(M,\omega)$-conjugacy class of Hamiltonian circle actions.

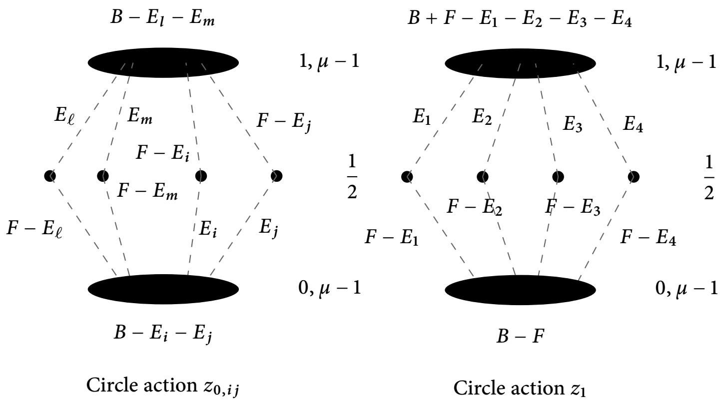

Figure 5: Family of graphs in the case $\mu > 1$.

Notice that these actions only exist as long as the symplectic area of the classes corresponding to the fixed spheres is positive. Assuming $1 < \mu \leq \frac{3}{2}$, we have four circle actions represented by the graphs in Figure 5. We can consider for example: $z_{0,12}, z_{0,13}, z_{0,14}$ and z_1. We do not consider flips of these graphs as they represent actions which are inverse to these ones.

Remark 4.1 Note that removing the homology labels and the dotted edges from the graphs representing the four actions $z_{0,12}, z_{0,13}, z_{0,14}$, and z_1, we get exactly the same underlying labeled graph. It follows that these four Hamiltonian circle actions are conjugated by symplectomorphisms that act nontrivially on homology.

Moreover, as we increase the value of μ, there are more classes that can be represented by the fixed spheres, as we see next. If we consider $\mu > \frac{3}{2}$, then we can add the graphs in Figure 6 to the previous family. It should be clear that there are eight such graphs, because $i, j, \ell, m = 1, 2, 3, 4$ are all distinct. More precisely, we have the graphs representing the following actions: $z_{0,123}, z_{0,124}, z_{0,134}, z_{0,234}$ and $z_{1,1}, z_{1,2}, z_{1,3}, z_{1,4}$.

Then there are no more possible classes for the fixed symplectic spheres unless we consider $\mu > 2$. In this case, eight new circle actions appear, where the following pairs of classes are represented by the fixed spheres: B and $B-E_1-E_2-E_3-E_4$; $B-2F$ and $B+2F-E_1-E_2-E_3-E_4$; and $B-F-E_i-E_j$ and $B+F-E_\ell-E_m$ with $i, j, \ell, m = 1, 2, 3, 4$ all distinct. If we restrict the range of values of μ further, it is easy to see that the number of circle actions keeps increasing. More precisely, when μ passes $k+\frac{1}{2}$ or $k+1$, for $k \in \mathbb{Z}_{\geq 1}$, the number of actions always increases by 8. Therefore, we obtain the following proposition.

Proposition 4.2 *The Hamiltonian circle actions on the symplectic manifolds belonging to the edge MA of the reduced symplectic cone are the ones represented by the labeled graphs in Figure 7. In particular, these actions satisfy the following existence*

https://doi.org/10.4153/S0008414X22000323 Published online by Cambridge University Press

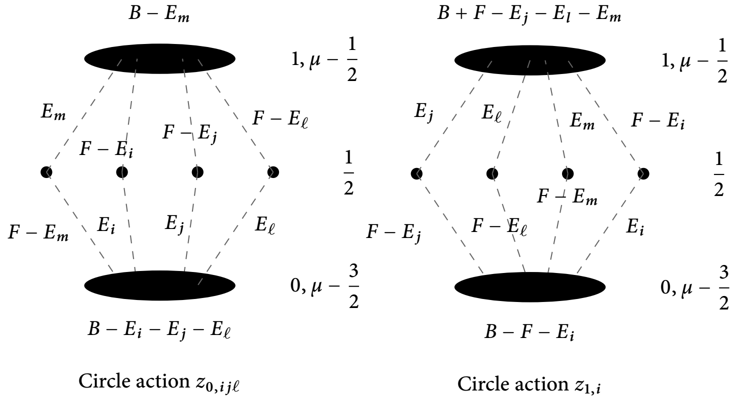

Figure 6: New family of graphs if $\mu > \frac{3}{2}$.

conditions:

- z_k *exists iff* $\mu > k$ *and* $\mu > 2 - k$,
- $z_{k,i}$ *exists iff* $\mu > k + \frac{1}{2}$ *and* $\mu > \frac{3}{2} - k$,
- $z_{k,ij}$ *exists iff* $\mu > k + 1$,
- $z_{k,ijl}$ *exists iff* $\mu > k + \frac{3}{2}$,
- $z_{k,1234}$ *exists iff* $\mu > k + 2$,

where $k \in \mathbb{Z}_{\geq 0}$ *and* $i, j, \ell, m = 1, 2, 3, 4$ *are all distinct.*

Remark 4.3 As we saw above, when $1 < \mu \leq \frac{3}{2}$, there exist only four Hamiltonian circle actions: $z_{0,12}, z_{0,13}, z_{0,14}$, and z_1, so there are not enough circle actions to generate the fundamental group. Then, when μ passes $k + \frac{1}{2}$, where $k \geq 1$, there exist eight more circle actions, namely $z_{k-1,123}, z_{k-1,124}, z_{k-1,134}, z_{k-1,234}$, and $z_{k,i}$ with $i = 1, 2, 3, 4$, and when μ passes $k + 1$, eight more circle actions appear: $z_{k-1,1234}$, $z_{k,12}, z_{k,13}, z_{k,14}, z_{k,23}, z_{k,24}, z_{k,34}$, and z_{k+1}.

Remark 4.4 Although the number of Hamiltonian circle actions keeps increasing as the values of μ increase, we know by the work of Li et al. in [18] that the rank of π_1 remains constant as μ increases so there can only be at most five independent circle actions as elements of the fundamental group.

Remark 4.5 In the forthcoming sections, we prove that, for $\mu > \frac{3}{2}$, the fundamental group $\pi_1(\mathrm{Symp}(M_{\mu,c_i=1/2})) \otimes \mathbb{Q}$ is indeed generated by circle actions. We choose as a tentative set of generators the set consisting of the four circle actions $z_{0,12}, z_{0,13}, z_{0,14}$, and z_1, which are the only ones that exist for all values of μ plus the action $z_{1,4}$, which exists as soon as μ passes $\frac{3}{2}$. The reason why we choose this action, among the new eight actions which appear when μ passes $\frac{3}{2}$, is geometric and relates with the work of

https://doi.org/10.4153/S0008414X22000323 Published online by Cambridge University Press

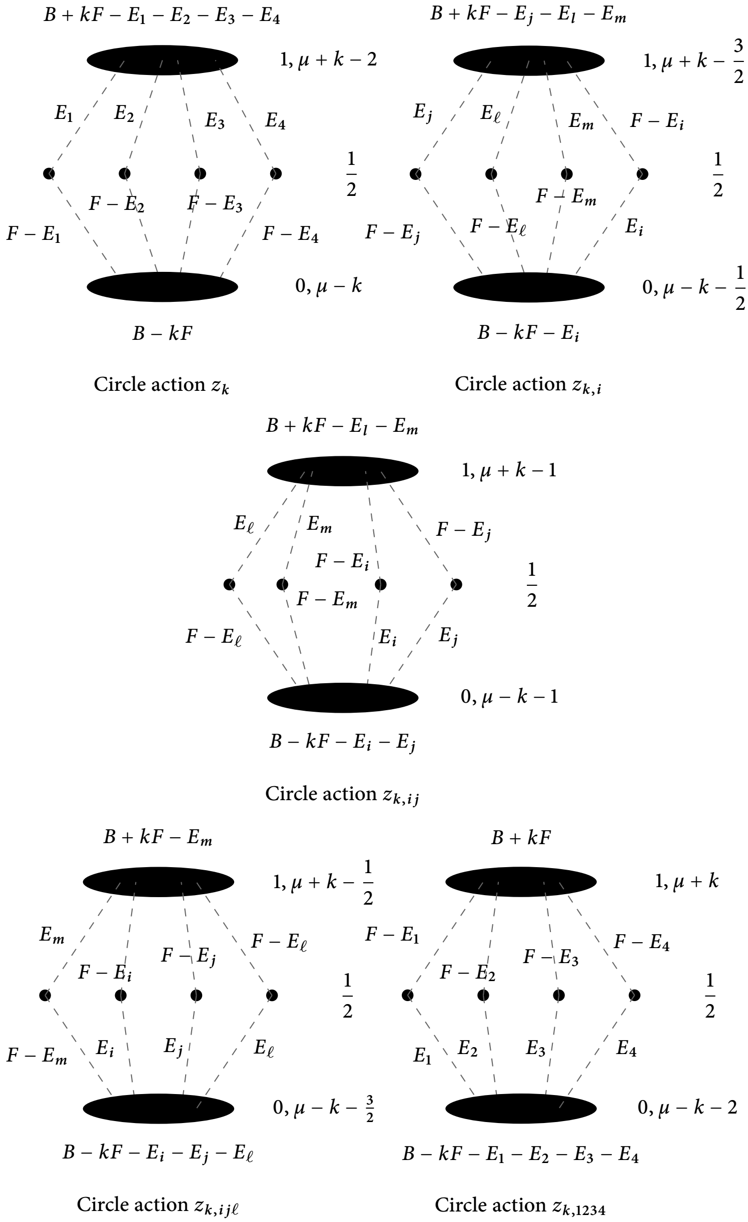

Figure 7: Families of graphs of Hamiltonian S^1-spaces encoded by the edge MA.

[18]. This action corresponds to a simultaneous rotation of all the spheres except the base in the configuration of seven exceptional spheres used in the proof of [18, Lemma 5.10], where the authors show that the rank of $\pi_1(\mathrm{Symp}_h(M_{\mu,c_i=1/2}))$ is 5. While the

https://doi.org/10.4153/S0008414X22000323 Published online by Cambridge University Press

first four actions fix spheres with self-intersection -2, the action $z_{1,4}$ fixes a -3 self-intersection sphere in class $B - F - E_4$.

4.4 The Seidel morphism along the edge MA

In this subsection, we prove our first main theorem, namely Theorem 1.3. The proof relies on the computation of the Seidel elements associated with the circle actions $z_{0,1i}$, $i = 2, 3, 4$, z_1, and $z_{1,4}$, and on the fact that they are linearly independent in the subgroup of invertible elements of the quantum homology of the manifold $M_{\mu,c_i=1/2}$.

4.4.1 Seidel elements and deformations

In order to describe the Seidel morphism

$$\mathcal{S} : \pi_1(\mathrm{Symp}(M_{\mu,c_i=1/2})) \to QH_{2n}(M_{\mu,c_i=1/2})^{\times},$$

our strategy is to combine the invariance property of $\mathcal{S}$ under the natural $\mathrm{Symp}_h(M, \omega)$ action, the invariance of Gromov–Witten invariants with respect to symplectic deformations, and Theorem 2.2, which describes certain Seidel elements associated with subcircles of toric actions on NEF symplectic manifolds.

More precisely, we first observe that the Seidel morphism

$$\mathcal{S} : \pi_1(\mathrm{Symp}_0(M, \omega)) \to QH_{2n}(M, \omega)^{\times}$$

defined in Section 2.2 is invariant under the action of $\pi_0(\mathrm{Symp}_h(M, \omega))$ on $\pi_1(\mathrm{Symp}_0(M, \omega)$. This follows from the definition of $\mathcal{S}$ and, in the case of Hamiltonian circle actions, can be seen directly from the formula (2.3) given by McDuff and Tolman. In particular, given a Hamiltonian circle action $\gamma : S^1 \to \mathrm{Ham}(M, \omega)$, its image $\mathcal{S}(\gamma)$ is determined by the labeled extended graph associated with γ.

Next, consider a Hamiltonian circle action ρ on $M_{\mu,c_i=1/2}$ and the corresponding loop $[\rho]$ in $\mathrm{Symp}(M_{\mu,c_i=1/2})$. Let $\Omega(\rho)$ be the space of all symplectic forms that are invariant under this action and write $\Omega_0(\rho)$ for the connected component of $\omega_{\mu,c_i=1/2}$. A $\mathbb{Q}$*-generic symplectic form* is a symplectic form whose cohomology class $[\mu; c_1, \ldots, c_4]$ is given by coefficients that are linearly independent over $\mathbb{Q}$. One can show that invariant $\mathbb{Q}$-generic symplectic forms are dense in $\Omega_0(\rho)$: let ω be any invariant symplectic form and δ_i be invariant closed two forms whose cohomology classes are a basis for $H^2(M, \mathbb{R})$. Then, for sufficiently small c_i, the two forms $\omega + \sum_i c_i \delta_i$ are invariant and symplectic. The result follows readily.

The same argument shows that extended graphs whose moment map labels are small continuous perturbations of the labels associated with ρ correspond to deformation equivalent symplectic forms invariant under the same circle action. Consequently, for any S^1-manifold (M, ω') associated with such an extended graph, there is no ambiguity as to what the Seidel element $\mathcal{S}([\rho]) \in QH_{2n}(M, \omega')^{\times}$ is.[1]

[1] In order to compare the Seidel homomorphisms associated with deformation-equivalent symplectic forms, a more general approach would be to use an enlarged Novikov ring as in [30].

We now observe that, due to deformation invariance of Gromov–Witten invariants, given any symplectic form ω' in $\Omega_0(\rho)$, the quantum homology ring $QH(M, \omega')$ is obtained from the quantum ring of a $\mathbb{Q}$-generic class $\omega_{\mu,c_1,c_2,c_3,c_4}$ by setting the values of the coefficients μ, c_1, c_2, c_3, c_4 equal to those of ω'. We thus have a natural specialization map $QH(M, \omega_{\mu,c_1,c_2,c_3,c_4}) \to QH(M, \omega')$, which sends the Seidel element of $[\rho]$ computed relatively to the generic form $\omega_{\mu,c_1,c_2,c_3,c_4}$ to the one computed relatively to the form ω'.

Finally, we can apply the previous discussion starting with a Hamiltonian circle actions ρ on $M_{\mu,c_i=1/2}$. From the above remarks, we can find a deformation equivalent $\mathbb{Q}$-generic form $\omega_{\mu;c_1,c_2,c_3,c_4}$ such that the sizes of the blowups satisfy the inequalities $0 < c_4 < c_3 < c_2 < c_1 < c_i + c_j < 1 < \mu$, with $i, j \in \{1, 2, 3, 4\}$ distinct. Symplectic cohomology classes satisfying this condition are said to be *reduced generic* or, more simply, *generic*. By choosing the sizes carefully, we can embed the circle action ρ into a toric action of a toric manifold that is NEF, and for which Theorem 2.2 applies. This allows us to compute the Seidel element of ρ.

In what follows, we consider Hamiltonian actions fixing spheres in the same homology classes as the ones in Proposition 4.2 and we list in Figure 8 their graphs. Note that we use the same notation for the circle actions in the generic case as, for the circle actions along the edge MA, we do not distinguish one case from the other with regard to notation.

4.4.2 Computing Seidel elements from toric actions

First, consider the actions $z_{0,12}, z_{0,13}, z_{0,14}$ and the polygon of Figure 9. The action $z_{0,12}$ corresponds to the circle action whose moment map is the first component of the moment map associated with the toric action $T_{0,12}$, represented in this figure. Moreover, it is clear that the homology classes of the fixed spheres are $B - E_1 - E_2$ and $B - E_3 - E_4$. Then Theorem 2.2(2a) yields

$$\mathcal{S}(z_{0,12}) = [B - E_3 - E_4] \otimes q \, \frac{t^{\varepsilon}}{1 - t^{c_3+c_4-\mu}},$$

where ε is the maximum of the momentum map of the action $z_{0,12}$, $\phi_{\max}(F_{\max})$, where $F_{\max}$ is the maximal 2-sphere whose momentum image is the edge in class $B - E_3 - E_4$, in the normalized polygon. In general, we obtain

$$\mathcal{S}(z_{0,1i}) = [B - E_j - E_\ell] \otimes q \, \frac{t^{\varepsilon}}{1 - t^{c_j+c_\ell-\mu}}, \quad \text{where} \quad j \neq \ell \neq i.$$

One can check that the normalized polygon yields

$$\varepsilon = \frac{c_j^3 + 3c_1^2 - c_1^3 + c_\ell^3 + 3c_i^2 - c_i^3 - 3\mu}{3(c_1^2 + c_2^2 + c_3^2 + c_4^2 - 2\mu)}.$$

Hence, if $c_i = 1/2$ for all i, we obtain $\varepsilon = 1/2$ and

$$\mathcal{S}(z_{0,1i}) = [B - E_j - E_\ell] \otimes q \, \frac{t^{\frac{1}{2}}}{1 - t^{1-\mu}}, \quad \text{where} \quad j \neq \ell \neq i. \tag{4.1}$$

Note that the expression is well defined because $\mu > 1$.

https://doi.org/10.4153/S0008414X22000323 Published online by Cambridge University Press

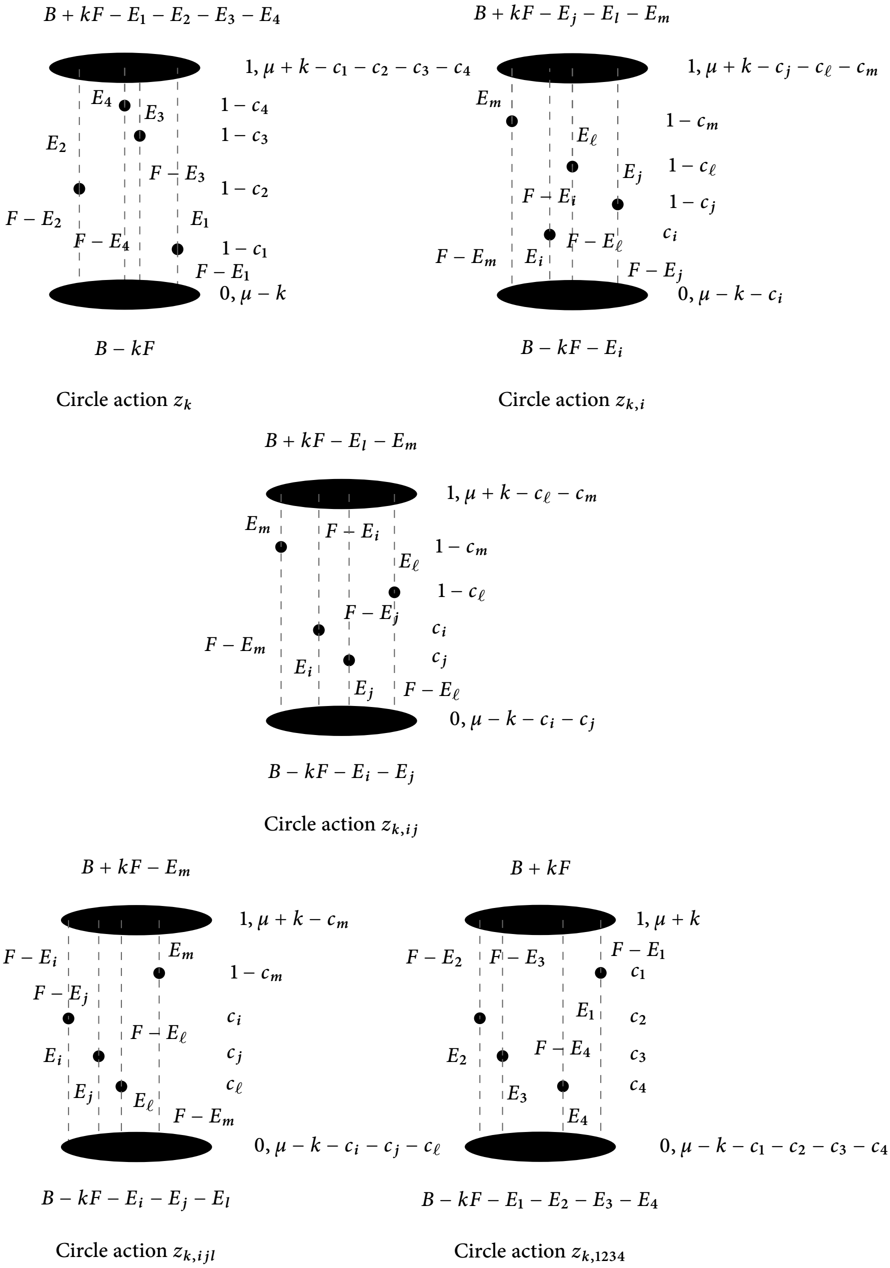

Figure 8: Graphs of the circle actions z_k, $z_{k,i}$, $z_{k,ij}$, $z_{k,ijl}$, and $z_{k,1234}$ in the generic case.

https://doi.org/10.4153/S0008414X22000323 Published online by Cambridge University Press

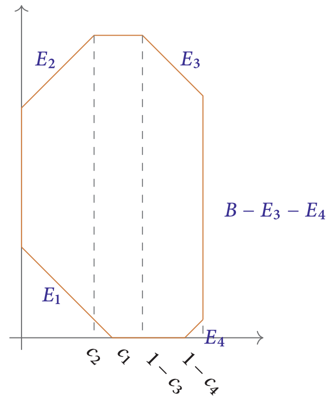

Figure 9: Toric action $T_{0,12}$.

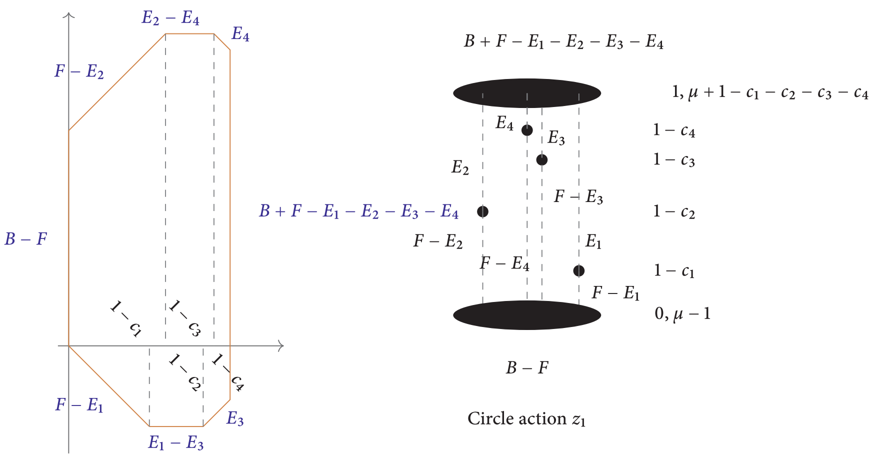

Figure 10: Toric action T_1 and its projection to the x-axis.

Consider now the polygon of Figure 10, which represents a toric action on M_{μ,c_1,c_2,c_3,c_4}, and for which the homology classes of the edges are represented in the figure. The graph of the circle action obtained by the projection of the polygon onto the x-axis is also represented in Figure 10. Note that it becomes the action z_1 defined in Figure 5 if $c_i=1/2$ for all i.

Now, Theorem 2.2(2a) gives

$$\mathcal{S}(z_1)=[B+F-E_1-E_2-E_3-E_4]\otimes q\,\frac{t^{1-\varepsilon}}{1-t^{c_1+c_2+c_3+c_4-\mu-1}},$$

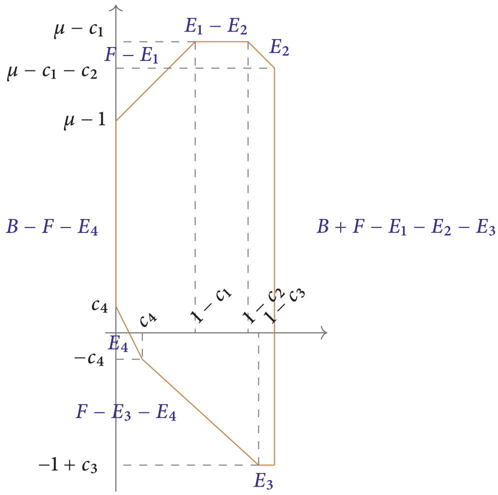

Figure 11: Toric action $(z_{1,4}, s_{1,4})$.

where in this case the maximum of the momentum map on the invariant sphere is given by

$$\varepsilon = \frac{-1 - c_1^3 + 3c_1^2 + 3c_2^2 - c_2^3 + 3c_3^2 - c_3^3 + 3c_4^2 - c_4^3 + 3c_1c_4^2 - 3c_3c_4^2 - 3\mu}{3(c_1^2 + c_2^2 + c_3^2 + c_4^2 - 2\mu)},$$

which is simply equal to $1/2$ if $c_i = 1/2$ for all i. Therefore, we obtain

$$\mathcal{S}(z_1) = [B + F - E_1 - E_2 - E_3 - E_4] \otimes q \frac{t^{\frac{1}{2}}}{1 - t^{1-\mu}}. \tag{4.2}$$

Finally, we compute the Seidel element of the circle action $z_{1,4}$, seen as an element of the fundamental group of $\mathrm{Symp}_h(M_{\mu,c_1,c_2,c_3,c_4})$. In order to do that, first consider the Delzant polygon of Figure 11. It represents a toric action on M_{μ,c_1,c_2,c_3,c_4} and its projections onto the x-axis and the y-axis are represented in Figure 12. Note that the projection onto the x-axis corresponds to the graph of the action $z_{1,4}$ given in Figure 6. Let us denote the action whose graph is obtained by projection onto the y-axis by $s_{1,4}$.

Since $c_1(B - F - E_4) = -1 < 0$, the complex manifold corresponding to Figure 11 is not NEF and we cannot apply immediately Theorem 2.2 to compute the Seidel element of $z_{1,4}$. Instead, we need to consider some auxiliary polygons for which the underlying complex manifolds are NEF and relate the circle actions represented on those polygons with the actions $z_{1,4}$ and $s_{1,4}$. More precisely, consider the Delzant polygon, on the left in Figure 13 and apply the $GL(2, \mathbb{Z})$ transformation represented by the matrix

$$\begin{pmatrix} 1 & 0 \\ 1 & 1 \end{pmatrix} \tag{4.3}$$

https://doi.org/10.4153/S0008414X22000323 Published online by Cambridge University Press

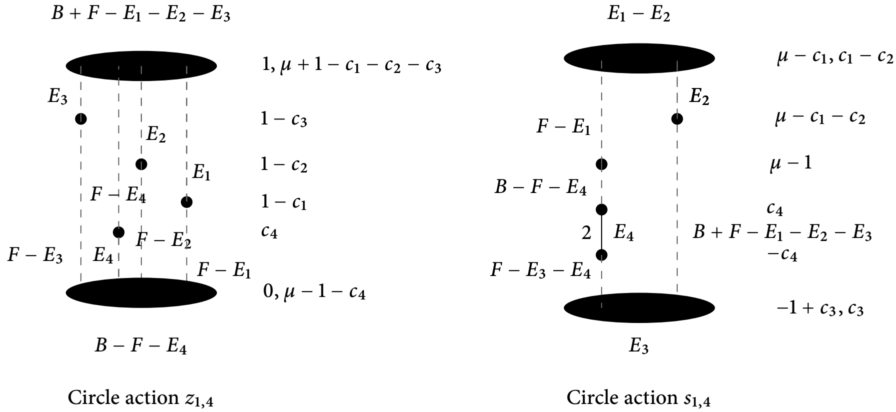

Figure 12: Graphs of circle actions $z_{1,4}$ and $s_{1,4}$, respectively.

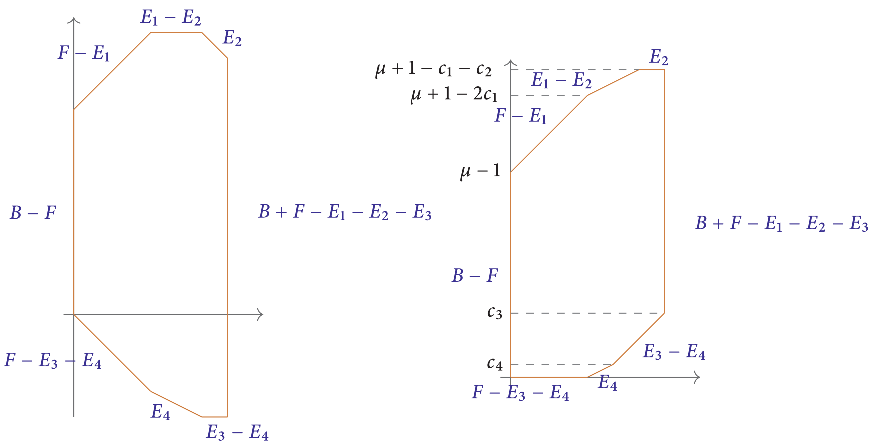

Figure 13: Polygon representing an NEF complex manifold and its transformation by the $GL(2, \mathbb{Z})$ matrix (4.3).

to this polygon as well as to the polygon of Figure 11. Then consider the projection onto the y-axis of the two transformed polygons and denote the action obtained this way from the polygon of Figure 13 by $t_{1,4}$. It is easy to check that the two graphs coincide, which implies that as elements of $\pi_1(\mathrm{Symp}_h(M_{\mu,c_1,c_2,c_3,c_4}))$ the following identification holds

$$z_{1,4} + s_{1,4} = t_{1,4}. \tag{4.4}$$

On the other hand, consider the polygon on the left in Figure 14, which represents a toric action, denoted by (x_1, y_1), on M_{μ,c_1,c_2,c_3,c_4} and its transformation by the same $GL(2, \mathbb{Z})$ matrix (4.3). The projection of the transformed polygon onto the y-axis

https://doi.org/10.4153/S0008414X22000323 Published online by Cambridge University Press

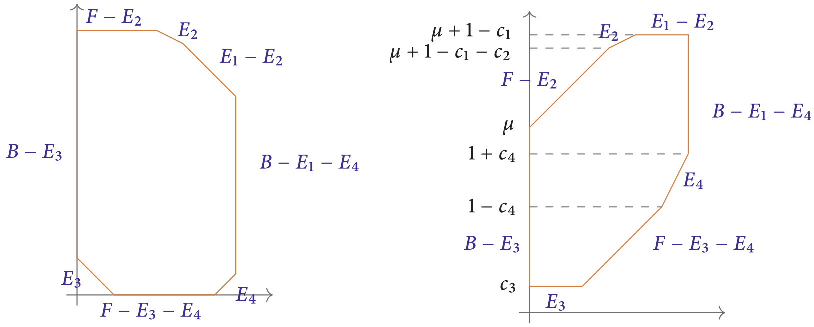

Figure 14: Toric action (x_1, y_1) and its transformation by the $GL(2,\mathbb{Z})$ matrix (4.3).

yields a graph that, up to translation, coincides with the graph of the action $s_{1,4}$, which implies that $s_{1,4} = x_1 + y_1$.

Note that, in Figure 14, we have $c_1(A) \geq 0$ for all homology classes A of the fixed spheres corresponding to edges of the polygon, so we can apply Theorem 2.2 to compute the Seidel element of $s_{1,4} = x_1 + y_1$. Moreover, it follows from equation (4.4) that the Seidel element of $z_{1,4}$ is given by

$$\mathcal{S}(z_{1,4}) = \mathcal{S}(t_{1,4})\mathcal{S}(s_{1,4})^{-1}. \tag{4.5}$$

More precisely, Theorem 2.2(3a) yields the Seidel elements of $t_{1,4}$ and $-s_{1,4}$, which are readable directly from the polygons on the right in Figures 13 and 14.

$$\mathcal{S}(t_{1,4}) = E_2 \otimes q t^{\mu+1-c_1-c_2-\gamma} - (E_1 - E_2) \otimes q \frac{t^{\mu+1-2c_1-\gamma}}{1 - t^{c_2-c_1}},$$
$$\mathcal{S}(s_{1,4})^{-1} = E_3 \otimes q t^{\beta-c_3} - (F - E_3 - E_4) \otimes q \frac{t^{\beta+c_4-1}}{1 - t^{c_3+c_4-1}},$$

where the exponents of the higher degree terms, namely of E_2 and E_3, are the maximal values of the momentum map for the normalized polygons. Therefore, one can check that

$$\gamma = \frac{-1 + 3c_1^2 - 3c_1^3 + 3c_2^2 - 3c_1c_2^2 - 2c_2^3 + c_3^3 + c_4^3 + 3c_1^2\mu + 3c_2^2\mu - 3\mu^2}{3(c_1^2 + c_2^2 + c_3^2 + c_4^2 - 2\mu)}$$

and

$$\beta = \frac{3c_1^2 - 2c_1^3 + 3c_2^2 - 3c_1c_2^2 - c_2^3 + 2c_3^3 + 3c_4^2 - 3\mu + 3c_1^2\mu + 3c_2^2\mu - 3\mu^2}{3(c_1^2 + c_2^2 + c_3^2 + c_4^2 - 2\mu)}.$$

Using [7, Proposition 5.3], we can now compute the quantum product (4.5) (we leave the details to the interested reader since it is a long and boring computation) and finally obtain

$$\mathcal{S}(z_{1,4}) = ((B + F - E_1 - E_2 - E_3) \otimes q + \mathbb{1} \otimes t^{c_4-\mu})t^{\beta-\gamma},$$

where the identity $\mathbb{1}$ is the homology class of the manifold, $[\mathbb{CP}^2\#5\overline{\mathbb{CP}^2}]\in H_4(\mathbb{CP}^2\#5\overline{\mathbb{CP}^2},\mathbb{Z})$. In what follows, we will suppress the identity from the expressions in order to simplify the notation.

If $c_i = 1/2$ for all i, then

$$\mathcal{S}(z_{1,4}) = ((B+F-E_1-E_2-E_3)\otimes q + t^{\frac{1}{2}-\mu})t^{\frac{2-3\mu}{3(1-2\mu)}}. \tag{4.6}$$

Note that this result agrees with McDuff–Tolman's result as the leading term is given by the homology class of the edge where the action is maximal.

Remark 4.6 In a similar way, we can compute the Seidel element of the inverse of $z_{1,4}$:

(4.7)
$$\mathcal{S}(z_{1,4})^{-1} = [(B-F-E_4)\otimes q + [pt]\otimes q^2\, t^{\frac{3}{2}-\mu} + (3F-E_1-E_2-E_3+E_4)\otimes q\, t^{1-\mu} + (B-E_4)\otimes q\, t^{2-2\mu} + t^{\frac{1}{2}-\mu}(1+t^{2-2\mu})]\frac{t^{\frac{1-3\mu}{3(1-2\mu)}}}{(1-t^{1-\mu})^4}.$$

Since all the possible Hamiltonian circle actions on $M_{\mu,c_i=1/2}$ have semi-free maximal sets, the McDuff–Tolman result always applies. Observe that, when $\mu > \frac{3}{2}$, the leading term is the homology class $B+F-E_4$, corresponding to the homology class of the edge where the moment map is maximal, in accordance with the McDuff–Tolman formula. Otherwise, if $1<\mu\le\frac{3}{2}$, the leading term is given by the class of a point, showing that the quantum homology class (4.7) is not the image of an effective Hamiltonian action under the Seidel homomorphism.

4.4.3 Injectivity of the Seidel morphism for $\mu > 3/2$

Proposition 4.7 *Consider the circle actions $z_{0,1i}$, $i=2,3,4$, z_1, and $z_{1,4}$, defined in Figure 7. If $\mu>\frac{3}{2}$ and $c_1=c_2=c_3=c_4=1/2$, then the Seidel elements of these five circle actions generate a free subgroup of rank 5 in the group of invertible elements of the quantum homology.* ■

Proof Using the notation of Section 3 for the quantum homology ring, the Seidel elements of these five circle actions are given by the following expressions:

$$\mathcal{S}(z_{0,12}) = b_{34},\quad \mathcal{S}(z_{0,13}) = b_{24},\quad \mathcal{S}(z_{0,14}) = b_{23}, \tag{4.8}$$

$$\mathcal{S}(z_1) = b_{12}+f_{34},\quad \mathcal{S}(z_{1,4}) = \left(b_{12}+f_{34}+e_4+\frac{t^{1-\mu}}{1-t^{1-\mu}}\right)(1-t^{1-\mu})\,t^{\frac{1}{6(1-2\mu)}}. \tag{4.9}$$

In order to show they are linearly independent, we first consider a simplification of the quantum algebra, namely, we set the b_{ij}, for all i,j, equal to an element b, the f_{ij} to f, and e_j to e. Then the quantum homology algebra becomes isomorphic to the Π^{univ}-algebra

$$\Pi^{\mathrm{univ}}[f,b,e]/I', \tag{4.10}$$

https://doi.org/10.4153/S0008414X22000323 Published online by Cambridge University Press

where I' is the ideal generated by

$$(1)\ f^2=0,\qquad (2)\ b^2=1,\qquad (3)\ f(b+1)=0,$$
$$(4)\ f\left(e+\frac{t^{1-\mu}}{1-t^{1-\mu}}\right)=0,\qquad (5)\ b\left(e+\frac{t^{1-\mu}}{1-t^{1-\mu}}\right)=f+e+\frac{t^{1-\mu}}{1-t^{1-\mu}},$$
$$(6)\ e^2=2(b+f+e)\frac{t^{1-\mu}}{1-t^{1-\mu}}+2\frac{t^{1-\mu}}{(1-t^{1-\mu})^2}+\frac{t^{2-2\mu}}{(1-t^{1-\mu})^2}.$$

Moreover, it is clear that the Seidel elements simplify to

$$\mathcal{S}(z_{0,12})=\mathcal{S}(z_{0,13})=\mathcal{S}(z_{0,14})=b,\quad \mathcal{S}(z_1)=b+f,$$
$$\text{and}\quad \mathcal{S}(z_{1,4})=\left(b+f+e+\frac{t^{1-\mu}}{1-t^{1-\mu}}\right)(1-t^{1-\mu})\,t^{\frac{1}{6(1-2\mu)}}.$$

We postpone the proof of the next two lemmas to Appendix A.

Lemma 4.8 *Consider the elements b, $b+f$, and $\left(b+f+e+\frac{t^{1-\mu}}{1-t^{1-\mu}}\right)(1-t^{1-\mu})\,t^{\frac{1}{6(1-2\mu)}}$ contained in the subgroup of invertible elements of the algebra $\Pi^{\text{univ}}[f,b,e]/I'$. They are linearly independent, that is, if*

$$b^{\alpha}(b+f)^{\beta}\left(b+f+e+\frac{t^{1-\mu}}{1-t^{1-\mu}}\right)^{\gamma}(1-t^{1-\mu})^{\gamma}\,t^{\frac{\gamma}{6(1-2\mu)}}=1,\quad \textit{where}\quad \alpha,\beta,\gamma\in\mathbb{Z},$$

then $\alpha=\beta=\gamma=0$. ■

Lemma 4.9 *The Seidel elements b_{34}, b_{24}, and b_{23} are linearly independent in the subgroup of invertible elements of the quantum homology $QH_4^{\times}(M_{\mu,c_i=1/2})$.*

Now, putting together the two lemmas, it is easy to conclude that the five Seidel elements $\mathcal{S}(z_{0,12}),\mathcal{S}(z_{0,13}),\mathcal{S}(z_{0,14}),\mathcal{S}(z_1)$, and $\mathcal{S}(z_{1,4})$ are linearly independent. If

$$\mathcal{S}(z_{0,12})^{\alpha_1}\,\mathcal{S}(z_{0,13})^{\alpha_2}\,\mathcal{S}(z_{0,14})^{\alpha_3}\,\mathcal{S}(z_1)^{\beta}\,\mathcal{S}(z_{1,4})^{\gamma}=1,$$

then

$$b_{34}^{\alpha_1}\,b_{24}^{\alpha_2}\,b_{23}^{\alpha_3}\,(b_{12}+f_{34})^{\beta}\left(b_{12}+f_{34}+e_4+\frac{t^{1-\mu}}{1-t^{1-\mu}}\right)^{\gamma}(1-t^{1-\mu})^{\gamma}\,t^{\frac{\gamma}{6(1-2\mu)}}=1.$$

Using the simplification above of the quantum homology algebra, one obtains

$$b^{\alpha_1+\alpha_2+\alpha_3}\,(b+f)^{\beta}\left(b+f+e+\frac{t^{1-\mu}}{1-t^{1-\mu}}\right)^{\gamma}(1-t^{1-\mu})^{\gamma}\,t^{\frac{\gamma}{6(1-2\mu)}}=1.$$

From Lemma 4.8, we conclude that $\alpha_1+\alpha_2+\alpha_3=\beta=\gamma=0$. Therefore,

$$b_{34}^{\alpha_1}\,b_{24}^{\alpha_2}\,b_{23}^{\alpha_3}=1,$$

and Lemma 4.9 implies that $\alpha_1=\alpha_2=\alpha_3=0$, so the five Seidel elements are linearly independent.

Next, we study the action of $\pi_0(\mathrm{Symp}_h(M,\omega))$ on $\pi_1(\mathrm{Symp}_0(M,\omega))$.

Proposition 4.10 *If (M,ω) belongs to the edge MA of the reduced symplectic cone, and if $\mu > 3/2$, then the Seidel homomorphism is injective and the action of $\pi_0(\mathrm{Symp}_h(M,\omega))$ on $\pi_1(\mathrm{Symp}_0(M,\omega))$ is trivial.* ■

Proof The Seidel homomorphism factors through

$$\begin{tikzcd} \pi_1(\mathrm{Symp}_0(M,\omega)) \arrow[rr, "\mathcal{S}"] \arrow[dr, "\pi"'] & & QH_{2n}(M,\omega)^\times \\ & \pi_1(\mathrm{Symp}_0(M,\omega))/\pi_0(\mathrm{Symp}_h(M,\omega)). \arrow[ur] & \end{tikzcd}$$

Consider arbitrary lifts in $\pi_1(\mathrm{Symp}_0(M,\omega)) \simeq \mathbb{Z}^5$ of the five actions. By Proposition 4.7, these lifts generate a free subgroup of rank 5 in $\pi_1(\mathrm{Symp}_0(M,\omega)) \simeq \mathbb{Z}^5$ on which the Seidel homomorphism $\mathcal{S}$ is injective. Consequently, $\mathcal{S}$ is injective on the whole group $\pi_1(\mathrm{Symp}_0(M,\omega))$. Since $\pi_1(\mathrm{Symp}_0(M,\omega))/\pi_0(\mathrm{Symp}_h(M,\omega))$ is also of rank 5, the triviality of the action follows readily. ■

Corollary 4.11 *Each labeled extended graph in Figures 5–7 corresponds to a well-defined homotopy class in $\pi_1(\mathrm{Symp}_0(M,\omega))$.*

We now prove Theorem 1.3.

Proof Consider the extended labeled graph $z_{0,1i}$, $i = 2,3,4$, z_1, and $z_{1,4}$ of Figure 7. It follows from Corollary 4.11 that these graphs define five elements of $\pi_1(\mathrm{Symp}_h(M_{\mu,c_i=1/2}))$. By Proposition 4.7, these five elements are linearly independent. This proves the second statement of the theorem. The first statement follows immediately from Remark 4.3. ■

Note that the proof of Proposition 4.7 does not depend on the value of μ, in addition to the condition $\mu > 1$. It follows that the five quantum homology classes b_{34}, b_{24}, b_{23}, $b_{12} + f_{34}$, and

$$\left(b_{12} + f_{34} + e_4 + \frac{t^{1-\mu}}{1-t^{1-\mu}}\right)(1-t^{1-\mu})\, t^{\frac{1}{6(1-2\mu)}} \tag{4.11}$$

generate a free subgroup of rank 5 in the group of invertible elements of the quantum homology, for every $\mu > 1$. This observation proves the following result.

Proposition 4.12 *When $1 < \mu \le \frac{3}{2}$, the quantum class (4.11) is not contained in the $\mathbb{Q}$-subspace spanned by circle actions inside the $\mathbb{Q}$-vector space formed by Seidel elements.* ■

4.5 Relations between Hamiltonian circle actions on M_{μ,c_1,c_2,c_3,c_4}

In this section, we prove our second main result. The main step is to obtain a classification of all circle actions in $\mathrm{Symp}_h(M_{\mu,c_i=1/2})$, which also shows that although we have more and more circle actions on $M_{\mu,c_i=1/2}$ as we increase the value of μ, they do not give new generators in the fundamental group of the symplectomorphism group $\mathrm{Symp}_h(M_{\mu,c_i=1/2})$. We show this by describing relations between the loops z_k,

https://doi.org/10.4153/S0008414X22000323 Published online by Cambridge University Press

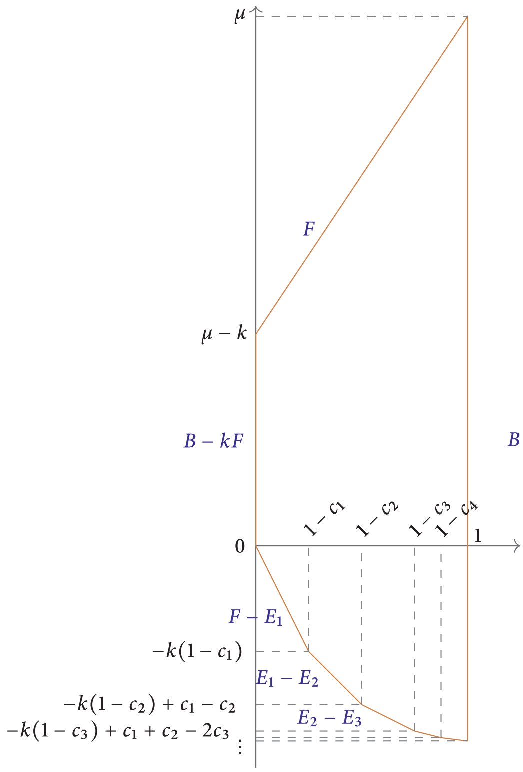

Figure 15: Toric action T_k.

$z_{k,i}$, $z_{k,ij}$, $z_{k,ijl}$, and $z_{k,1234}$, described in Section 4.3, that come from embedding pairs of loops inside torus actions. The tools we use are Delzant's classification of toric actions and Karshon's classification of Hamiltonian circle actions. We always consider the actions in the generic case, that is, when $0 < c_4 < c_3 < c_2 < c_1 < c_i + c_j < 1 < \mu$, with $i, j \in \{1, 2, 3, 4\}$, in order to obtain the relations between the loops. As explained in Section 4.4.1, these relations between actions induce relations between Seidel elements in the quantum ring associated with the generic symplectic form. These relations map to similar relations in the quantum homology ring of $M_{\mu,c_i=1/2}$. By injectivity of the Seidel homomorphism when $\mu > 3/2$, we deduce that these relations hold in $\pi_1(\mathrm{Symp}(M_{\mu,c_i=1/2}))$ as well.

Consider the manifold M_{μ,c_1,c_2,c_3,c_4} endowed with a toric action, which we denote by T_k, such that the momentum polygon is given in Figure 15. In addition to the homology classes indicated in the figure, it should be clear that the classes $E_3 - E_4$ and E_4 are also represented in the bottom edges. Projecting onto the x-axis and the y-axis, we obtain the graphs in Figure 16 of the actions z_k and w_k, respectively, whose momentum maps are the first and second coordinates of the momentum map of the action T_k.

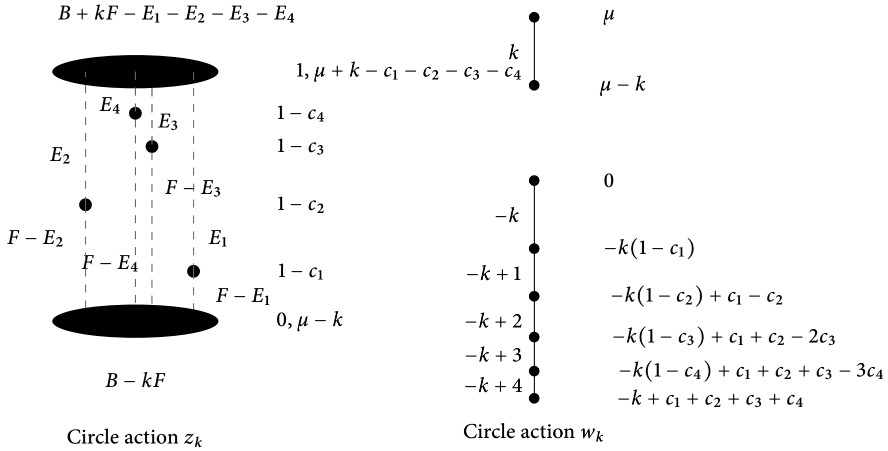

Figure 16: Graphs of the circle actions z_k and w_k, respectively.

Performing the $GL(2,\mathbb{Z})$ transformation represented by the matrix

$$\begin{pmatrix} 1 & 0 \\ j & -1 \end{pmatrix}$$

to the polygon of Figure 15 yields a new polygon representing the same toric manifold. This new polygon has vertices

$(1, j - \mu)$, $(0, k - \mu)$, $(0,0)$, $(1 - c_1, (j + k)(1 - c_1))$, $(1 - c_2, (j + k)(1 - c_2) - c_1 + c_2)$, $(1 - c_3, (j + k)(1 - c_3) - c_1 - c_2 + 2c_3)$, $(1 - c_4, (j + k)(1 - c_4) - c_1 - c_2 - c_3 + 3c_4)$, and $(1, j + k - c_1 - c_2 - c_3 - c_4)$.

Then perform the $GL(2,\mathbb{Z})$ transformation represented by the matrix

$$\begin{pmatrix} 1 & 0 \\ k & -1 \end{pmatrix}$$

to the polygon of the toric action T_j. It should be clear, looking at the coordinates of the two transformed polygons, that projecting both polygons onto the y-axis, we obtain the same graph, which implies that

$$jz_k - w_k = kz_j - w_j, \quad j,k \geq 1. \tag{4.12}$$

Now, consider the toric action T_0 on M_{μ,c_1,c_2,c_3,c_4} represented in the Delzant polygon of Figure 17. Consider also its projections, in Figure 18, to the x-axis and the y-axis representing circle actions that we denote by (z_0, y_0).

Again, performing the $GL(2,\mathbb{Z})$ transformation represented by the matrix

$$\begin{pmatrix} 1 & 0 \\ -k & 1 \end{pmatrix}$$

https://doi.org/10.4153/S0008414X22000323 Published online by Cambridge University Press

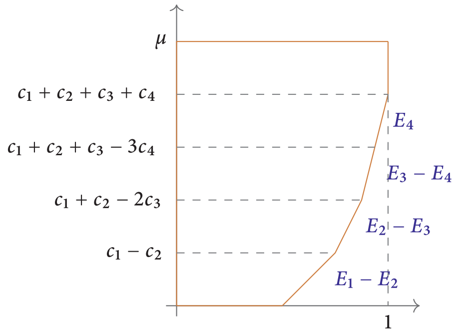

Figure 17: Toric action T_0.

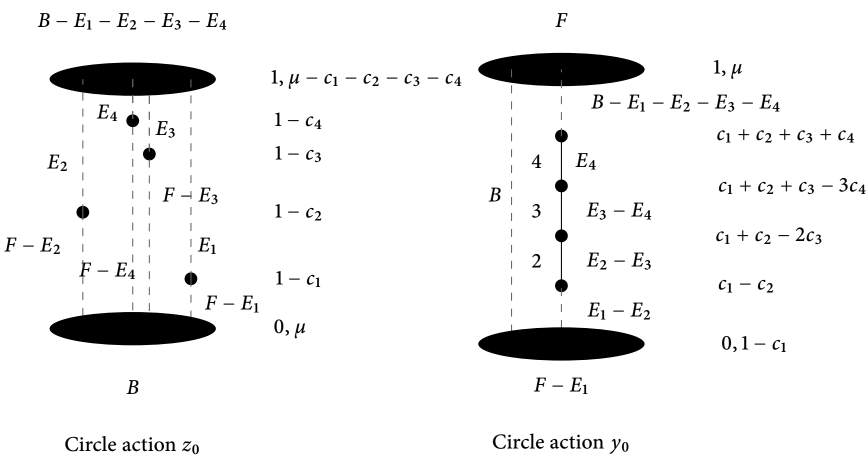

Figure 18: Graphs of circle actions z_0 and y_0, respectively.

to the polygon of Figure 17 yields a new polygon representing the same toric manifold. This new polygon has vertices

$$(0,\mu),(1,\mu-k),(0,0),(1-c_1,-k(1-c_1)),(1-c_2,-k(1-c_2)+c_1-c_2),$$
$$(1-c_3,-k(1-c_3)+c_1+c_2-2c_3),(1-c_4,-k(1-c_4)+c_1+c_2+c_3-3c_4),\ \text{and}$$
$$(1,-k+c_1+c_2+c_3+c_4).$$

Therefore, projecting this new polygon onto the y-axis, it is easy to check that we obtain the graph of the circle action w_k, which means we have the following identification:

$$w_k = -kz_0 + y_0, \qquad k \geq 1. \tag{4.13}$$

Combining equations (4.12) and (4.13) yields

$$jz_k + kz_0 = kz_j + jz_0.$$

https://doi.org/10.4153/S0008414X22000323 Published online by Cambridge University Press

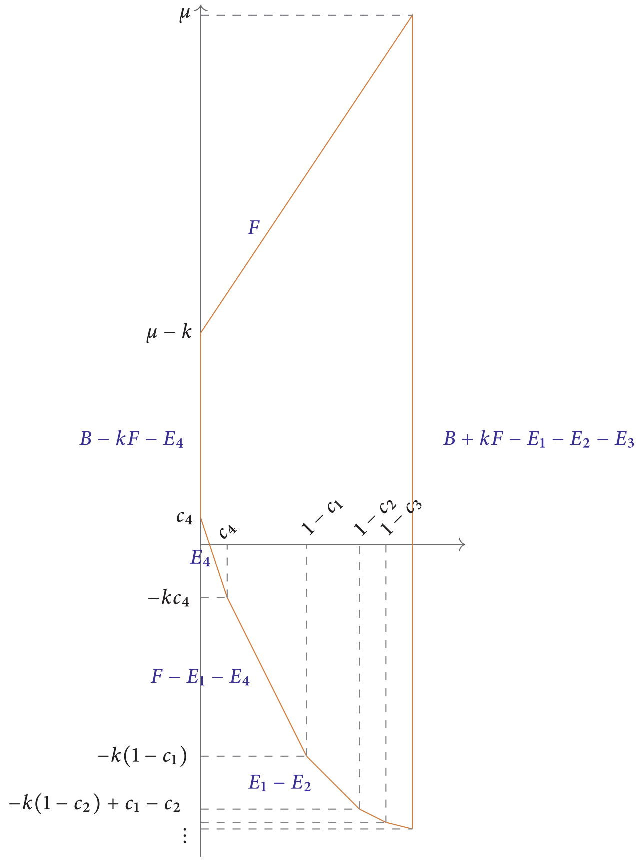

Figure 19: Toric action $T_{k,4}$.

Finally, setting $j = 1$ implies that

$$z_k = kz_1 + (1-k)z_0, \quad k \geq 0. \tag{4.14}$$

Next, we use a similar argument in order to obtain more relations between other circle actions listed in Proposition 4.2. For that, we need to consider the toric action $T_{k,4}$ on M_{μ,c_1,c_2,c_3,c_4}, represented in the momentum polytope in Figure 19. Note that the two edges without homology labels represent the classes, $E_2 - E_3$ and E_3.

Projecting onto the x- and y-axes, we obtain the graphs in Figure 20 of the actions $(z_{k,4}, w_{k,4})$, respectively, whose momentum maps are the first and second coordinates of the momentum map of the action $T_{k,4}$.

Using the same argument as before, that is, performing the $GL(2,\mathbb{Z})$ transformation represented by the following matrix

$$\begin{pmatrix} 1 & 0 \\ j & -1 \end{pmatrix}$$

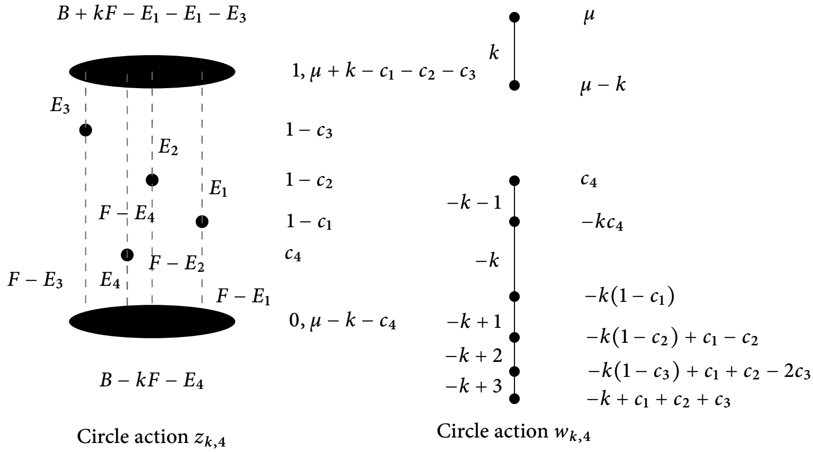

Figure 20: Graphs of the circle actions $z_{k,4}$ and $w_{k,4}$.

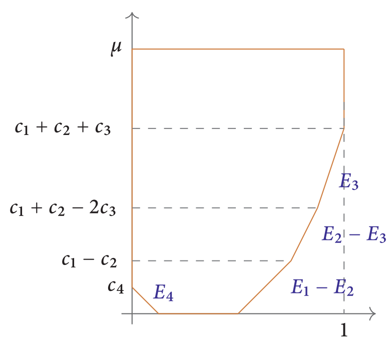

Figure 21: Toric action $T_{0,4}$.

on the polygon of Figure 19 yields a new polygon with vertices

$(1, j + k - c_1 - c_2 - c_3), (1, j - \mu), (0, k - \mu), (0, -c_4), (c_4, (j+k)c_4), (1 - c_1, (j+k)(1 - c_1)),$
$(1 - c_2, (j+k)(1 - c_2) - c_1 + c_2)$, and $(1 - c_3, (j+k)(1 - c_3) - c_1 - c_2 + 2c_3)$.

Interchanging the role of k and j and then projecting onto the y-axis, it follows that

$$jz_{k,4} - w_{k,4} = kz_{j,4} - w_{j,4}, \qquad j, k \geq 1. \tag{4.15}$$

Now, consider the toric action on M_{μ,c_1,c_2,c_3,c_4} represented in the polygon of Figure 21. Consider also its projections, in Figure 22, to the x- and y-axes representing circle actions that we denote by $(z_{0,4}, y_{0,4})$.

In this case, performing the $GL(2,\mathbb{Z})$ transformation represented by the matrix

$$\begin{pmatrix} 1 & 0 \\ -k & 1 \end{pmatrix}$$

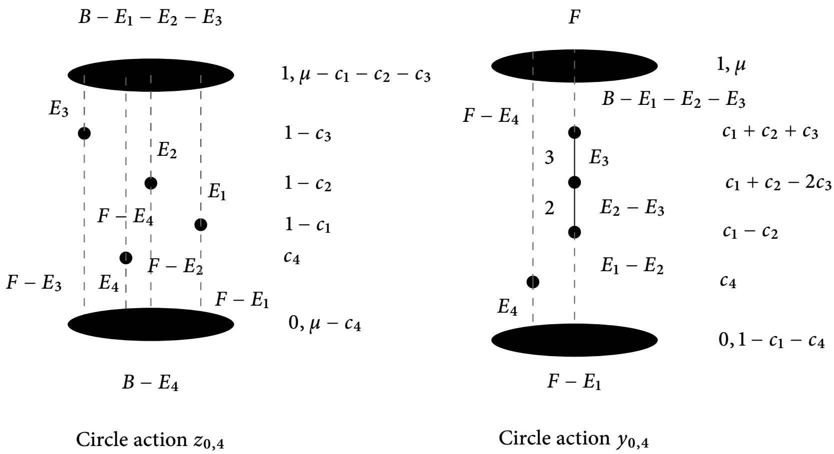

Figure 22: Graphs of the circle actions $z_{0,4}$ and $y_{0,4}$, respectively.

to the polygon of Figure 21 yields a new polygon whose vertices are

$$(0,\mu), (1,\mu-k), (0,c_4), (c_4,-kc_4), (1-c_1,-k(1-c_1)), (1-c_2,-k(1-c_2)+c_1-c_2),$$
$$(1-c_3,-k(1-c_3)+c_1+c_2-2c_3), \text{ and } (1,-k+c_1+c_2+c_3).$$

Therefore, projecting this new polygon onto the y-axis, it is clear that one obtains the graph of the circle action $w_{k,4}$, which means we have the following relation:

$$w_k = -kz_{0,4} + y_{0,4}, \quad k \geq 1. \tag{4.16}$$

Combining equations (4.15) and (4.16) yields

$$jz_{k,4} + kz_{0,4} = kz_{j,4} + jz_{0,4},$$

and setting $j = 1$ implies that

$$z_{k,4} = kz_{1,4} + (1-k)z_{0,4}, \quad k \geq 0.$$

Therefore, it is clear that, in fact, we have the following identifications:

$$z_{k,i} = kz_{1,i} + (1-k)z_{0,i}, \quad k \geq 0, \quad i = 1,2,3,4. \tag{4.17}$$

Using a similar argument three more times applied to the appropriate toric actions on the manifold M_{μ,c_1,c_2,c_3,c_4}, it follows that the following identifications hold:

$$z_{k,ij} = kz_{1,ij} + (1-k)z_{0,ij}, \quad k \geq 0, \quad i,j = 1,2,3,4, \tag{4.18}$$

(4.19)
$$z_{k,ij\ell} = kz_{1,ij\ell} + (k-1)z_{0,m}, \quad k \geq 0, \quad i,j,\ell,m = 1,2,3,4, \quad \text{and all indices are distinct;}$$

and

$$z_{k,1234} = kz_{1,1234} + (k-1)z_0, \quad k \geq 0. \tag{4.20}$$

https://doi.org/10.4153/S0008414X22000323 Published online by Cambridge University Press

In what follows, we will often use the next proposition. The proof follows from techniques similar to the ones used to obtain the previous relations, so we postpone it to Appendix B.

Proposition 4.13 *Consider the circle actions z_0, $z_{0,i}$, $i = 1,2,3,4$, $z_{0,1i}$, $i = 2,3,4$, z_1, and $z_{1,4}$, defined in Figure 7 or 8 through their graphs, as elements of $\pi_1(\mathrm{Symp}_h(M_{\mu,c_1,c_2,c_3,c_4}))$. Then the following identifications hold:*

$$z_{0,1} = z_1 - z_{1,4} + z_{0,14}, \qquad z_{0,2} = z_1 - z_{1,4} - z_{0,13},$$
$$z_{0,3} = z_1 - z_{1,4} - z_{0,12}, \qquad z_{0,4} = z_1 - z_{1,4} - z_{0,12} - z_{0,13} + z_{0,14},$$

and $z_0 = 2z_1 - 2z_{1,4} - z_{0,12} - z_{0,13} + z_{0,14}$. ∎

Putting together Proposition 4.13 with equations (4.14) and (4.17)–(4.20), we then obtain the following result.

Proposition 4.14 *Consider the circle actions $z_{0,1i}$, $i = 2,3,4$, z_1, and $z_{1,4}$, defined in Figure 7 or 8 through their graphs, as elements of $\pi_1(\mathrm{Symp}_h(M_{\mu,c_1,c_2,c_3,c_4}))$. Let $t = z_{0,12} + z_{0,13} - z_{0,14}$. Then, for $k \in \mathbb{Z}_{\geq 0}$ and $i, j = 1,2,3,4$ with $i \neq j$, we have the following identifications:*

$$z_k = (2-k)z_1 + (k-1)(2z_{1,4} + t), \qquad z_{k,ij} = 2kz_{1,4} - kz_1 + kt + z_{0,ij},$$
$$z_{k,1} = (2k-1)z_{1,4} + (1-k)z_1 + kt + z_{0,14}, \qquad z_{k,124} = (2k+1)z_{1,4} - (k+1)z_1 + kt + z_{0,12},$$
$$z_{k,2} = (2k-1)z_{1,4} + (1-k)z_1 + kt - z_{0,13}, \qquad z_{k,134} = (2k+1)z_{1,4} - (k+1)z_1 + kt + z_{0,13},$$
$$z_{k,3} = (2k-1)z_{1,4} + (1-k)z_1 + kt - z_{0,12}, \qquad z_{k,234} = (2k+1)z_{1,4} - (k+1)z_1 + kt - z_{0,14},$$
$$z_{k,4} = (2k-1)z_{1,4} + (1-k)z_1 + (k-1)t, \qquad z_{k,123} = (2k+1)z_{1,4} - (k+1)z_1 + (k+1)t,$$

and $z_{k,1234} = (2k+2)z_{1,4} - (k+2)z_1 + (k+1)t$. ∎

Remark 4.15 It is clear from the definition of the circle actions $z_{0,ij}$ that

$$z_{0,ij} = -z_{0,kl}.$$

Thus, we get

$$z_{23} = -z_{0,14}, \quad z_{24} = -z_{0,13}, \quad z_{34} = -z_{0,12},$$

which allows us to write $z_{k,ij}$ completely in terms of the chosen generators.

Corollary 4.16 *If $\mu > \frac{3}{2}$, then there are loops in $\pi_1(\mathrm{Symp}(M_{\mu,c_i=1/2}))$ which are not represented by circle actions, although the fundamental group, rationally, is generated by circle actions.*

Proof We use the classification of all circle actions on $\mathrm{Symp}(M_{\mu,c_i=1/2})$ obtained in Proposition 4.14 to show that those actions do not fill in the lattice $\mathbb{Z}^5$. In fact, it is sufficient to look at the plane of the actions $z_{1,4}$ and z_1. There we have five families of points defined by the pairs $(2k-2, 2-k)$, $(2k-1, 1-k)$, $(2k, -k)$, $(2k+1, -(k+1))$, and $(2k+2, -(k+2))$. Each family is contained in one line with slope $-\frac{1}{2}$, whereas the y-intercepts are given by $1, \frac{1}{2}, 0, -\frac{1}{2}$, and -1, respectively. We should also consider the integer multiples of these actions as they represent circle actions although they are not effective. The corresponding points lie in lines connecting the origin to the points representing the effective actions. The set of all these points clearly do not fill in the

https://doi.org/10.4153/S0008414X22000323 Published online by Cambridge University Press

full lattice $\mathbb{Z}^2$ in this plane. For example, the primitive point $(2,3)$ is not contained in this set. Therefore, there are elements in π_1 which cannot be represented by circle actions. ■

We now prove Theorem 1.5.

Proof In the case $1<\mu\leq\frac{3}{2}$, it follows from Theorem 1.3, and in the case $\mu>\frac{3}{2}$, it follows from Corollary 4.16. ■

5 Further questions

In this paper, we deal with a particular case in the symplectic cone of M_{μ,c_1,c_2,c_3,c_4}, namely the edge MA, when $\mu>1$ and $c_i=1/2$ for all $i\in\{1,2,3,4\}$. A very natural question is whether there are other points in the symplectic cone where the fundamental group of $\mathrm{Symp}_h(M_{\mu,c_1,c_2,c_3,c_4})$ is not generated Hamiltonian circle actions, similarly to what happens along some points of the edge MA. For example, it is possible to check that, along the edge MD, where $\mu=1, c_1=c_2=c_3=1/2>c_4$, there are no circle actions. On the one hand, there are no graphs representing Hamiltonian S^1-spaces along this edge. However, the graph only encodes equivariant blowups. Not having such graphs does not a priori rule out the possibility of *exotic* circle actions, obtained by equivariant blowups corresponding to parameters $\mu', c_1', c_2', c_3', c_4'$ such that the symplectic manifold corresponding to these parameters is symplectomorphic to the symplectic manifold corresponding to the parameters μ, c_1, c_2, c_3, c_4. On the other hand, *exotic* circle actions were ruled out, first, by Pinsonnault in [26] and later by Karshon, Kessler, and Pinsonnault in [12]. Note that if we forget the fourth blowup, this case corresponds to the monotone case in $\mathrm{Symp}_h(S^2\times S^2\#3\overline{\mathbb{CP}}^2)$ and it is well known that there are no Hamiltonian circle actions in this case. In fact, this symplectomorphism group is contractible (see [9]). However, by the work of [18], we know that the rank of the fundamental group of $\mathrm{Symp}(M_{\mu,c_1,c_2,c_3,c_4})$ along the edge MD is 5, so none of these five generators can be represented by circle actions. Moreover, we believe that there is a neighborhood of the monotone point M, including points in the generic case, such that the generators of the fundamental group of $\mathrm{Symp}(M_{\mu,c_1,c_2,c_3,c_4})$ cannot all be realized by circle actions. The main reason appears to be that one circle action of the type $z_{0,i}$ or $z_{1,i}$ for some $i\in\{1,2,3,4\}$ always have to be included in the set of generators, in order to have the required number of generators, but this implies that there must exist a fixed sphere with positive area in class $B-E_j-E_k-E_\ell$ or $B-F-E_i$, that is, $\mu-c_j-c_k-c_\ell>0$ or $\mu-1-c_i>0$, respectively. However, this condition does not necessarily hold for all points in the symplectic cone, in particular, for points close to the monotone point M.

An alternative way of proving that there is an element of $\pi_1(\mathrm{Symp}_h(M_{\mu,c_1,c_2,c_3,c_4}))$ which cannot be represented by a circle action would be to compute the Samelson product of this loop with itself and check if it is nonzero, as done by Buse in [6, Proposition 3.3] (if it was generated by a circle action, this Samelson product would be trivially 0). Moreover, it would be interesting to know if this loop in π_1 gives rise to new elements in higher homotopy groups, via iterated Samelson products. The problem with this approach is that it is not clear yet how to obtain the necessary information about the higher homotopy groups of $\mathrm{Symp}_h(M_{\mu,c_1,c_2,c_3,c_4})$, which is fundamental to work on these ideas. The answer to these questions will be pursued in a different paper.

In another direction, it seems very likely that Theorem 1.4 holds not only rationally but also in the integer case, that is,

Conjecture 5.1 *If $\mu > \frac{3}{2}$, then the fundamental group $\pi_1(\mathrm{Symp}(M_{\mu,c_i=1/2}))$ is generated by Hamiltonian circle actions.* ∎

In fact, it is possible to show that the Seidel elements of the classes of the actions $z_{0,12}$, $z_{0,13}$, $z_{0,14}$, z_1, and $z_{1,4}$, seen as elements of $\pi_1(\mathrm{Symp}(M_{\mu,c_i=1/2}))$, are primitive in the subgroup of invertible elements of the quantum homology of $\mathrm{Symp}(M_{\mu,c_i=1/2})$. This result together with a geometric interpretation of the generators of $\pi_1(\mathrm{Symp}(M_{\mu,c_i=1/2}))$ given in [18, Lemma 5.10] might lead to a proof of this conjecture. We believe that this should involve a detailed analysis of the strata of the space of almost complex structures and the generators of their homology groups.

A Computations on the quantum ring

In this section, we prove Lemmas 4.8 and 4.9.

Proof (of Lemma 4.8) Recall that we wish to prove that the invertible elements b, $b+f$, and $\left(b+f+e+\frac{t^{1-\mu}}{1-t^{1-\mu}}\right)(1-t^{1-\mu})\,t^{\frac{1}{6(1-2\mu)}}$ are linearly independent in the subgroup of invertible elements of the ring (4.10). Suppose that

$$b^{\alpha}\,(b+f)^{\beta}\left(b+f+e+\frac{t^{1-\mu}}{1-t^{1-\mu}}\right)^{\gamma}(1-t^{1-\mu})^{\gamma}\,t^{\frac{\gamma}{6(1-2\mu)}}=1,\quad \text{where}\quad \alpha,\beta,\gamma\in\mathbb{Z}.$$

Using the relations in the ideal I' in (4.10), in particular relations (3) and (5), it follows that this is equivalent to

$$b^{\alpha}\,b^{\beta}(1-f)^{\beta}\,b^{\gamma}\left(e+\frac{1}{1-t^{1-\mu}}\right)^{\gamma}(1-t^{1-\mu})^{\gamma}\,t^{\frac{\gamma}{6(1-2\mu)}}=1 \iff$$

$$b^{\alpha+\beta+\gamma}\,(1-f)^{\beta}\,(e(1-t^{1-\mu})+1)^{\gamma}=t^{\frac{-\gamma}{6(1-2\mu)}} \iff$$

$$b^{\alpha+\beta+\gamma}\,(1-\beta f)\,(e(1-t^{1-\mu})+1)^{\gamma}=t^{\frac{-\gamma}{6(1-2\mu)}},$$

because $f^2=0$. Moreover, since $(1-\beta f)(1+\beta f)=1$, if $\alpha+\beta+\gamma$ is even, then we obtain

$$(e(1-t^{1-\mu})+1)^{\gamma}=(1+\beta f)\,t^{\frac{-\gamma}{6(1-2\mu)}}. \tag{A.1}$$

If $\gamma\geq 0$, then it should be clear from relations in I', in particular, from relation (6), that we cannot never obtain the right-hand side of the last expression, since it is not possible to obtain such power on t, unless $\gamma=0$, which implies that $\beta=0$ and then $\alpha=0$. If $\gamma\leq 0$, then equation (A.1) is equivalent to

$$(e(1-t^{1-\mu})+1)^{-\gamma}=(1-\beta f)\,t^{\frac{\gamma}{6(1-2\mu)}},$$

https://doi.org/10.4153/S0008414X22000323 Published online by Cambridge University Press

and again we can conclude that $\gamma = 0$. Similarly, if $\alpha+\beta+\gamma$ is odd, we obtain

$$(e(1-t^{1-\mu})+1)^{\gamma} = (b-\beta f)\, t^{\frac{-\gamma}{6(1-2\mu)}},$$

and again we can conclude that $\gamma=\beta=0$ and $\alpha+\beta+\gamma$ cannot be odd. This concludes the proof of the lemma. ∎

Proof (of Lemma 4.9) We first prove by induction on $n\in\mathbb{N}$ that

$$b_{ij}^{2n} = n(2n\,b_{ij}f_{ij} + (2n-1)f_{ij} + f_{k\ell}) + 1, \tag{A.2}$$

$$b_{ij}^{2n+1} = -n(2(n+1)b_{ij}f_{ij} + (2n+1)f_{ij} + f_{k\ell}) + b_{ij}, \tag{A.3}$$

where $i,j,k,\ell\in\{1,2,3,4\}$ are all distinct.

Note that if $n=1$, then (A.2) gives $b_{ij}^2 = 2b_{ij}f_{ij} + 1f_{ij} + f_{k\ell}$, which agrees with relation (3) in Proposition 3.1. Moreover, it follows from relation (3) together with relations (8) and (11) that

$$\begin{aligned}
b_{ij}^2 f_{ij} &= 2b_{ij}f_{ij}^2 + f_{ij}^2 + f_{ij}f_{k\ell} + f_{ij}\\
&= -f_{ij}^2 + f_{ij}\\
&= -2b_{ij}f_{ij} - f_{ij}.
\end{aligned}$$

Now, if we assume (A.2), then the previous equation together with relation (11) yields

$$\begin{aligned}
b_{ij}^{2(n+1)} &= b_{ij}^{2n}\, b_{ij}\\
&= n(2n\,b_{ij}^2 f_{ij} + (2n-1)f_{ij}b_{ij} + f_{k\ell}b_{ij}) + b_{ij} =\\
&= n(2n(-2b_{ij}f_{ij} - f_{ij}) + (2n-1)f_{ij}b_{ij} - f_{ij}b_{ij} - f_{ij} - f_{k\ell}) + b_{ij}\\
&= -n(2(n+1)b_{ij}f_{ij} + (2n+1)f_{ij} + f_{k\ell}) + b_{ij}.
\end{aligned}$$

Similarly, it is easy to check that

$$b_{ij}^{2n+1}b_{ij} = (n+1)(2(n+1)\,b_{ij}f_{ij} + (2n+1)f_{ij} + f_{k\ell}) + 1.$$

Next, using (A.2) and (A.3), we compute $b_{ij}^{\alpha_1}\,b_{ik}^{\alpha_2}\,b_{jk}^{\alpha_3}$, where $\alpha_1,\alpha_2,\alpha_3\in\mathbb{Z}$, to conclude that indeed b_{ij}, b_{ik}, b_{jk} are linearly independent. Assume first that $\alpha_1,\alpha_2,\alpha_3\geq 0$ and, in particular, $\alpha_i = 2n_i$, with $n_i\in\mathbb{N}_0$. Then

$$b_{ij}^{\alpha_1}\,b_{ik}^{\alpha_2} = [n_1(2n_1\,b_{ij}f_{ij} + (2n-1)f_{ij} + f_{k\ell}) + 1]\,[n_2(2n_2\,b_{ik}f_{ik} + (2n-1)f_{ik} + f_{j\ell}) + 1].$$

Recall relation (4) in Proposition 3.1: $b_{ij}f_{ik} = -f_{ik}$. This yields

$$\begin{aligned}
b_{ij}^{\alpha_1}\,b_{ik}^{\alpha_2} &= 4n_1^2\,n_2^2\,f_{ij}f_{ik} - n_2(2n_2-1)2n_1^2\,f_{ij}f_{ik} - n_1(2n_1-1)2n_2^2\,f_{ij}f_{ik} - 2n_1^2\,n_2\,f_{ij}f_{j\ell}\\
&\quad + 2n_1^2\,b_{ij}f_{ij} + n_1(2n_1-1)\,n_2(2n_2-1)\,f_{ij}f_{ik} + n_1(2n_1-1)\,n_2 f_{ij}f_{j\ell} + n_1(2n_1-1)\,f_{ij}\\
&\quad - 2n_1\,n_2^2\,f_{ik}f_{k\ell} + n_1\,n_2(2n_2-1)\,f_{ik}f_{k\ell} + n_1\,n_2\,f_{k\ell}f_{j\ell} + n_1\,f_{k\ell} + 2n_2^2\,b_{ik}f_{ik}\\
&\quad + n_2(2n_2-1)\,f_{ik} + n_2\,f_{j\ell} + 1\\
&= n_1\,n_2(f_{ij}f_{ik} - f_{ij}f_{j\ell} - f_{ik}f_{k\ell} + f_{k\ell}f_{j\ell}) + 2\,n_1^2 b_{ij}f_{ij} + 2\,n_2^2 b_{ik}f_{ik} + n_1(2n_1-1)\,f_{ij}\\
&\quad + n_2(2n_2-1)\,f_{ik} + n_1\,f_{k\ell} + n_2\,f_{j\ell} + 1\\
&= 2\,n_1^2 b_{ij}f_{ij} + 2\,n_2^2(b_{ij}f_{ij} + e_k - e_j) + n_1(2n_1-1)\,f_{ij} + n_2(2n_2-1)\,(f_{ij} + e_j - e_k)
\end{aligned}$$

$$+ n_1(f_{ij} + e_i + e_j - e_k - e_l) + n_2(f_{ij} + e_i - e_l) + 1$$
$$= 2(n_1^2 + n_2^2) f_{ij}(b_{ij} + 1) + e_i(n_1 + n_2) + e_j(n_1 - n_2) - e_k(n_2 - n_1) - e_\ell(n_1 + n_2) + 1,$$

where the step before the last follows from relations (2) and (9) in Proposition 3.1 and the definition of f_{ij} and e_i. Similar computations then give

$$b_{ij}^{\alpha_1} b_{ik}^{\alpha_2} b_{jk}^{\alpha_3} = 2(n_1^2 + n_2^2 + n_3^2) f_{ij}(b_{ij} + 1) + e_i(n_1 + n_2 - n_3) + e_j(n_1 - n_2 + n_3) + e_k(n_3 + n_2 - n_1) - e_\ell(n_1 + n_2 + n_3) + 1.$$

Now, it is clear that $b_{ij}^{\alpha_1} b_{ik}^{\alpha_2} b_{jk}^{\alpha_3} = 1$ iff $n_1 = n_2 = n_3 = 0$. In the case $\alpha_1 = 2n_1 + 1$, $\alpha_2 = 2n_2$, and $\alpha_3 = 2n_3$, analog computations yield

$$b_{ij}^{\alpha_1} b_{ik}^{\alpha_2} b_{jk}^{\alpha_3} = -2(n_1^2 + n_2^2 + n_3^2 + n_1) f_{ij}(b_{ij} + 1) - e_i(n_1 + n_2 - n_3) - e_j(n_1 - n_2 + n_3) - e_k(n_3 + n_2 - n_1) + e_\ell(n_1 + n_2 + n_3) + b_{ij}.$$

If $\alpha_1 = 2n_1 + 1$, $\alpha_2 = 2n_2 + 1$, and $\alpha_3 = 2n_3$, then

$$b_{ij}^{\alpha_1} b_{ik}^{\alpha_2} b_{jk}^{\alpha_3} = [2(n_1^2 + n_2^2 + n_3^2 + n_1 + n_2) + 1] f_{ij}(b_{ij} + 1) + e_i(n_1 + n_2 - n_3 + 1) + e_j(n_1 - n_2 + n_3) + e_k(n_3 + n_2 - n_1) - e_\ell(n_1 + n_2 + n_3 + 1) + 1.$$

Finally, if $\alpha_i = 2n_i + 1$, one obtains

$$b_{ij}^{\alpha_1} b_{ik}^{\alpha_2} b_{jk}^{\alpha_3} = -[2(n_1^2 + n_2^2 + n_3^2 + n_1 + n_2 + n_3) + 1] f_{ij}(b_{ij} + 1) - e_i(n_1 + n_2 - n_3) - e_j(n_1 - n_2 + n_3) - e_k(n_3 + n_2 - n_1 + 1) - e_\ell(n_1 + n_2 + n_3 + 1) + b_{ij}.$$

So it follows that $b_{ij}^{\alpha_1} b_{ik}^{\alpha_2} b_{jk}^{\alpha_3} = 1$ iff $\alpha_i = 0$ for all i.

If $\alpha_m < 0$, then we obtain similar expressions because $b_{ij}^{\alpha_m} = b_{k\ell}^{-\alpha_m}$. More precisely, in the case $\alpha_m > 0$, the products above contain the term $n_m(e_i + e_j - e_k - e_\ell)$, but if $\alpha_m < 0$, it is not hard to check that then the term is replaced by its symmetric $n_m(-e_i - e_j + e_k + e_\ell)$. Therefore, we prove that the elements b_{ij}, b_{ik}, b_{jk} are linearly independent, and, in particular, we finish the proof of Lemma 4.9. ∎

B Proof of Proposition 4.13

This section is devoted to a proof of Proposition 4.13. First, we need to prove that the following identifications hold.

Lemma B.1 *Consider the Hamiltonian circle actions $z_0, z_{0,1i}, z_{0,j}, z_1$, and $z_{1,4}$, where $i \in \{2,3,4\}$ and $j \in \{1,2,3,4\}$, whose graphs are represented in Figure 8, as elements of the fundamental group of* $\mathrm{Symp}_h(M_{\mu,c_1,c_2,c_3,c_4})$. *Then we have the following relations:*

$$z_1 + z_{0,4} = z_{1,4} + z_0, \tag{B.1}$$

$$z_0 = z_{0,3} + z_{0,4} + z_{0,12}, \tag{B.2}$$

$$z_{0,1} = z_{0,14} + z_{0,12} + z_{0,3}, \tag{B.3}$$

$$z_{0,2} = z_{0,12} - z_{0,13} + z_{0,3}, \tag{B.4}$$

$$z_{0,4} = z_{0,14} - z_{0,13} + z_{0,3}. \tag{B.5}$$

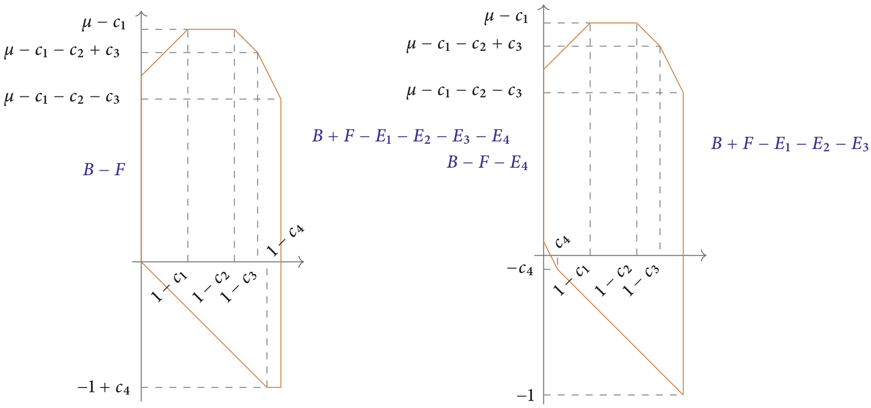

Figure 23: Auxiliary toric actions.

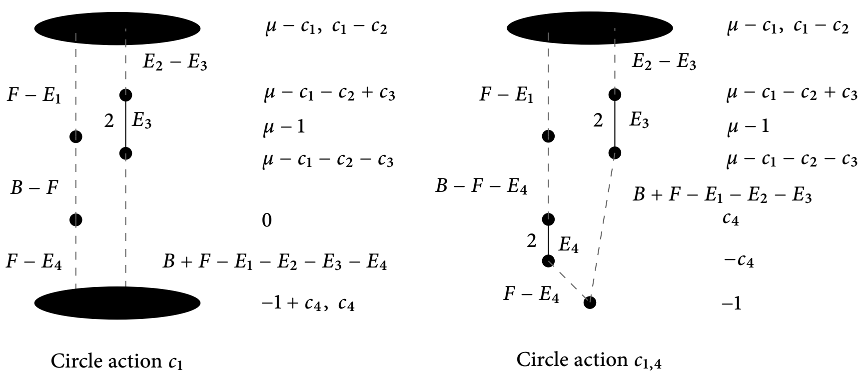

Figure 24: Graphs of the actions c_1 and $c_{1,4}$.

Proof In order to prove relation (B.1), we need to consider the two toric actions on M_{μ,c_1,c_2,c_3,c_4} represented in the polygons of Figure 23.

Note that, projecting onto the x-axis, we obtain the graphs of the circle actions z_1 on the left and $z_{1,4}$ on the right. On the other hand, projecting onto the y-axis yields the graphs of two circle actions (see Figure 24) that we will denote by c_1 and $c_{1,4}$.

It is easy to check that performing first a $GL(2,\mathbb{Z})$ transformation represented by the matrix

$$\begin{pmatrix} 1 & 0 \\ 1 & 1 \end{pmatrix}$$

to both polygons of Figure 23 and then a projection onto the y-axis, we obtain the same graph, which implies that the following identification holds:

$$z_1 + c_1 = z_{1,4} + c_{1,4}. \tag{B.6}$$

https://doi.org/10.4153/S0008414X22000323 Published online by Cambridge University Press

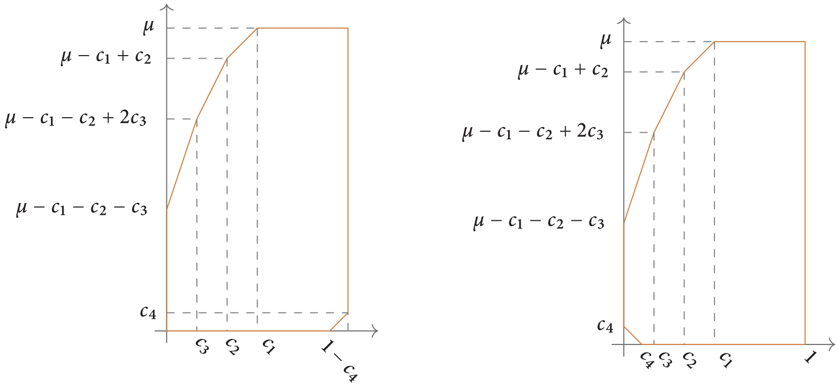

Figure 25: Toric actions (a_1, b_1) and $(a_{1,4}, b_{1,4})$.

Next, consider the polygons of Figure 25. Again, they represent particular toric actions on M_{μ,c_1,c_2,c_3,c_4}. We denote the circle actions whose graphs are obtained by projecting to the x- and y-axes by (a_1, b_1) and $(a_{1,4}, b_{1,4})$. Since, clearly, the actions b_1 and $b_{1,4}$ are represented by the same graph, it follows that $b_1 = b_{1,4}$. Next, performing a $GL(2,\mathbb{Z})$ transformation represented by the matrix

$$\begin{pmatrix} 1 & 0 \\ -1 & 1 \end{pmatrix}$$

to both polygons and then projecting to the y-axis, we obtain the graphs of c_1 and $c_{1,4}$. Therefore, as elements of $\pi_1(\mathrm{Symp}_h(M_{\mu,c_1,c_2,c_3,c_4}))$, the following identifications hold:

$$b_1 - a_1 = c_1 \quad \text{and} \quad b_{1,4} - a_{1,4} = c_{1,4}.$$

On the other hand, note that a_1 is the generator $-z_{0,4}$, whereas $a_{1,4}$ is $-z_0$. Therefore, we have

$$b_1 + z_{0,4} = c_1 \quad \text{and} \quad b_{1,4} + z_0 = c_{1,4}.$$

Finally, substituting c_1 and $c_{1,4}$ in relation (B.6) and using $b_1 = b_{1,4}$, we obtain the desired relation (B.1).

In order to prove the remaining relations in this lemma, we use an argument involving several auxiliary polygons representing different toric actions on M_{μ,c_1,c_2,c_3,c_4} that can be related between each other using Karshon's and Delzant's classifications. Since the argument is similar for all relations, we give the proof for relation (B.2) and leave the other proofs for the interested reader.

First, consider the toric actions on M_{μ,c_1,c_2,c_3,c_4} represented in the polygons of Figure 26. Denote the toric action in polygon $n \in \{1,2,3,4,5,6\}$ in Figure 26 by (x_n, y_n). Projecting onto the x-axis to obtain the graph of x_n, using Karshon's classification of Hamiltonian circle actions, it is clear that

(B.7) $$x_1 = x_2 = x_3 \quad \text{and} \quad x_4 = x_5.$$

https://doi.org/10.4153/S0008414X22000323 Published online by Cambridge University Press

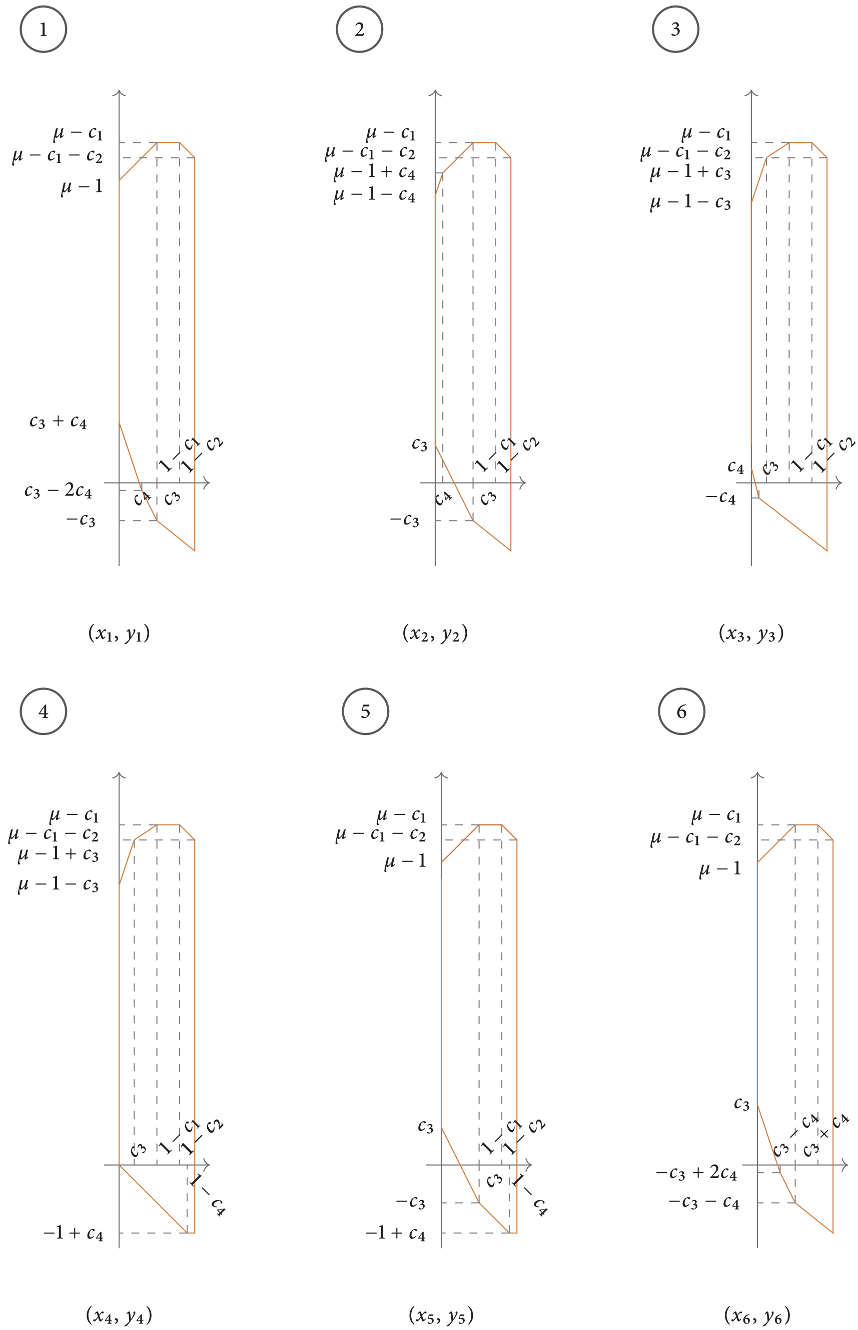

Figure 26: Auxiliary Delzant polygons.

https://doi.org/10.4153/S0008414X22000323 Published online by Cambridge University Press

Moreover, applying the $GL(2,\mathbb{Z})$ transformation represented by the matrix

$$\begin{pmatrix} 1 & 0 \\ 1 & 1 \end{pmatrix}$$

to the polygons 3, 4, 5, and 6 and then projecting onto the y-axis, it is easy to check that, as elements of the fundamental group, the following identifications hold:

$$x_3 + y_3 = x_4 + y_4, \tag{B.8}$$

$$x_5 + y_5 = x_6 + y_6. \tag{B.9}$$

Furthermore, the $GL(2,\mathbb{Z})$ transformation represented by the matrix

$$\begin{pmatrix} 1 & 0 \\ 2 & 1 \end{pmatrix}$$

applied to the polygons 1 and 6 yields, after a projection onto the y-axis and a comparison of the graphs obtained, the following relation:

$$2x_1 + y_1 = 2x_6 + y_6. \tag{B.10}$$

Next, consider the toric actions on M_{μ,c_1,c_2,c_3,c_4} represented in the polygons of Figure 27 and denote the toric action of polygon $n \in \{1,2,3,4,5,6\}$ by (s_n, t_n). Applying to all these polygons, the $GL(2,\mathbb{Z})$ transformation represented by the matrix

$$\begin{pmatrix} 1 & 0 \\ -1 & 1 \end{pmatrix}$$

and then projecting onto the y-axis, it is easy to see that we obtain, as elements of the fundamental group of $\mathrm{Symp}(M_{\mu,c_1,c_2,c_3,c_4})$, the following identification:

$$y_i = t_i - s_i, \quad i \in \{1,2,3,4,5,6\}, \tag{B.11}$$

because the graphs obtained after the projection clearly coincide with the graphs of the actions y_i. It is also clear that

$$t_3 = t_4 \quad \text{and} \quad t_5 = t_6, \tag{B.12}$$

since the graphs of these actions coincide in pairs. Finally, using the $GL(2,\mathbb{Z})$ transformation represented by the matrix

$$\begin{pmatrix} 1 & 0 \\ 1 & 1 \end{pmatrix}$$

applied to polygons 1 and 6 in Figure 27, we obtain the following identification:

$$s_1 + t_1 = s_6 + t_6. \tag{B.13}$$

In order to finish the proof of relation (B.2), we just need to combine all the relations obtained above. More precisely, consider relation (B.10) and using first (B.11) and then (B.13), we get

$$x_1 - s_1 = x_6 - s_6.$$

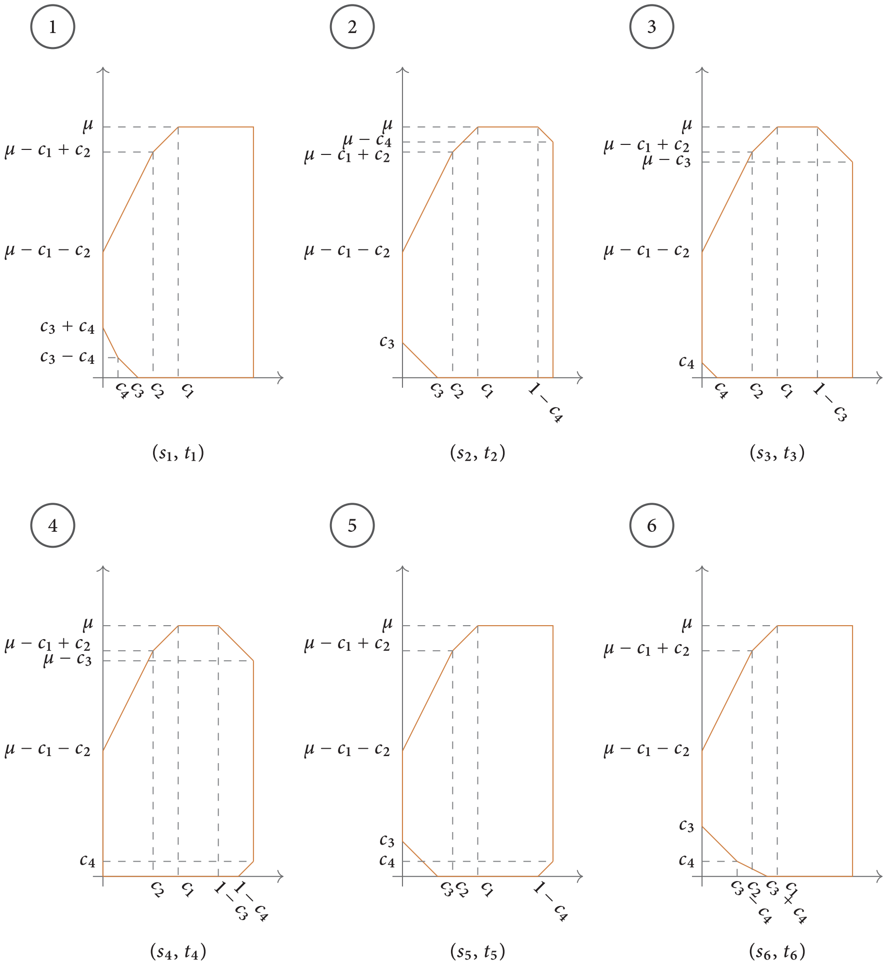

Figure 27: Auxiliary Delzant polygons.

From (B.7) and (B.9), it follows that $x_3 - s_1 = x_5 + y_5 - y_6 - s_6$. Then, using (B.11) to substitute y_5 and y_6 in the previous equation yields $x_3 - s_1 = x_5 + t_5 - s_5 - t_6$. Hence, relations (B.7) and (B.12) imply that $x_3 - s_1 = x_4 - s_5$. Finally, use first relation (B.8) to obtain $y_4 - y_3 = s_1 - s_5$ and then (B.11) one more time to get

$$s_3 - s_4 = s_1 - s_5.$$

Now, notice that, using the notation for the circle actions defined in Figure 8, we have

$$s_3 = -z_{0,3}, \quad s_4 = z_{0,12}, \quad s_1 = -z_0, \quad \text{and} \quad s_5 = -z_{0,4},$$

so we proved the desired relation (B.2). This concludes the proof of the lemma. ■

https://doi.org/10.4153/S0008414X22000323 Published online by Cambridge University Press

Combining relations (B.1) and (B.2), we obtain one of the identifications in Proposition 4.13, namely

$$z_{0,3} = z_1 - z_{1,4} - z_{0,12}. \tag{B.14}$$

The remaining identifications in Proposition 4.13 follow from the previous relation together with relations (B.3)–(B.5). Therefore, we obtain

$$\begin{aligned} z_{0,1} &= z_1 - z_{1,4} + z_{0,14}, \\ z_{0,2} &= z_1 - z_{1,4} - z_{0,13}, \\ z_{0,4} &= z_1 - z_{1,4} - z_{0,12} - z_{0,13} + z_{0,14}. \end{aligned}$$

Finally, using the last equation and relation (B.14) in relation (B.2), it follows that

$$z_0 = 2z_1 - 2z_{1,4} - z_{0,12} - z_{0,13} + z_{0,14}.$$

This concludes the proof of Proposition 4.13.

Acknowledgment The first and third authors are very grateful to Jun Li, Tian-Jun Li, and Weiwei Wu for showing and explaining to them their results in a preliminary version of [18]. The first author would also like to warmly thank Dusa McDuff for useful and enlightening discussions. The second and fourth authors kindly thank the support of the Gulbenkian Foundation which gave them the opportunity to take part on this work. Finally, we would like to thank the referees for their hard and thorough work in reviewing the paper. We greatly appreciate their comments and questions. Moreover, we think that the modifications based on their suggestions and corrections have vastly improved the paper.

References

[1] M. Abreu, G. Granja, and N. Kitchloo, *Compatible complex structures on symplectic rational ruled surfaces*. Duke Math. J. **148**(2009), 539–600.

[2] M. Abreu and D. McDuff, *Topology of symplectomorphism groups of rational ruled surfaces*. J. Amer. Math. Soc. **13**(2000), 971–1009.

[3] S. Anjos and S. Eden, *The homotopy Lie algebra of symplectomorphisms groups of 3-folds blow-ups of* $(S^2 \times S^2, \sigma_{\mathrm{std}} \oplus \sigma_{\mathrm{std}})$. Michigan Math. J. **68**(2019), no. 1, 71–126.

[4] S. Anjos and R. Leclercq, *Seidel's morphism of toric 4-manifolds*. J. Symplectic Geom. **16**(2018), no. 1, 1–68.

[5] S. Anjos and M. Pinsonnault, *The homotopy Lie algebra of symplectomorphism groups of 3-fold blow-ups of the projective plane*. Math. Z. **275**(2013), 245–292.

[6] O. Buse, *Negative inflation and stability in symplectomorphism groups of ruled surfaces*. J. Symplectic Geom. **9**(2011), no. 2, 147–160.

[7] B. Crauder and R. Miranda, *Quantum cohomology of rational surfaces*. In: R. H. Dijkgraaf, C. F. Faber, and G. B. M. van der Geer (eds.), The moduli space of curves. Progress in Mathematics, 129, Birkhäuser, Boston, 1995.

[8] T. Delzant, *Hamiltoniens périodiques et image convexe de l'application moment*. Bull. Soc. Math. France **116**(1988), 315–339.

[9] J. D. Evans, *Symplectic mapping class groups of some Stein and rational surfaces*. J. Symplectic Geom. **9**(2011), no. 1, 45–82.

[10] Y. Karshon, *Periodic Hamiltonian flows on four dimensional manifolds*, Memoirs of the American Mathematical Society, 141, no. 672 (1999).

[11] Y. Karshon and L. Kessler, *Distinguishing symplectic blowups of the complex projective plane*. J. Symplectic Geom. **15**(2017), no. 4, 1089–1128.

[12] Y. Karshon, L. Kessler, and M. Pinsonnault, *Counting Toric actions on symplectic four-manifolds*. C. R. Math. Acad. Sci. Soc. R. Can. **37**(2015), no. 1, 33–40.
[13] J. Kędra, *Fundamental group of* $Symp(M,\omega)$ *with no circle action*. Arch. Math. (Brno) **45**(2009), no. 1, 75–78.
[14] F. Lalonde and D. McDuff, *The classification of ruled symplectic 4-manifolds*. Math. Res. Lett. **3**(1996), 769–778.
[15] F. Lalonde and D. McDuff. *J-curves and the classification of rational and ruled symplectic 4-manifolds*. In: Contact and symplectic geometry (Cambridge, 1994), Publications of the Newton Institute, 8, Cambridge University Press, Cambridge, 1996, pp. 3–42 (in English summary).
[16] J. Li and T. J. Li, *Symplectic-2 spheres and the symplectomorphism group of small rational 4-manifolds*. Pacific J. Math. **304**(2020), no. 2, 561–606.
[17] J. Li, T. J. Li, and W. Wu, *The symplectic mapping class group of* $\mathbb{CP}^2\#n\overline{\mathbb{CP}^2}$ *with* $n \le 4$. Michigan Math. J. **64**(2015), no. 2, 319–333.
[18] J. Li, T. J. Li, and W. Wu, *Symplectic-2 spheres and the symplectomorphism group of small rational 4-manifolds II*. Trans. Amer. Math. Soc. **375**(2022), no. 2, 1357–1410.
[19] T. J. Li and A. Liu, *Symplectic structure on ruled surfaces and a generalized adjunction formula*. Math. Res. Lett. **2**(1995), no. 4, 453–471.
[20] T. J. Li and A. Liu, *Uniqueness of symplectic canonical class, surface cone and symplectic cone of 4-manifolds with* $b^+ = 1$. J. Differential Geom. **58**(2001), no. 2, 331–370.
[21] T. J. Li and W. Wu, *Lagrangian spheres, symplectic surfaces and the symplectic mapping class group*. Geom. Topol. **16**(2012), no. 2, 1121–1169.
[22] D. McDuff, *From symplectic deformation to isotopy*. In: Topics in symplectic 4-manifolds (Irvine, CA, 1996), International Press, Cambridge, MA, 1998, pp. 85–99.
[23] D. McDuff and D. A. Salamon, *J-holomorphic curves and quantum cohomology*. 2nd ed., American Mathematical Society Colloquium Publications, 52, American Mathematical Society, Providence, RI, 2012, xiv+726 pp.
[24] D. McDuff and S. Tolman, *Topological properties of Hamiltonian circle actions*. Int. Math. Res. Not. IMRN **2006**(2006), 72826.
[25] M. Pinsonnault, *Symplectomorphism groups and embeddings of balls into rational ruled surfaces*. Compos. Math. **144**(2008), no. 3, 787–810.
[26] M. Pinsonnault, *Maximal compact tori in the Hamiltonian group of 4-dimensional symplectic manifolds*. J. Mod. Dyn. **2**(2008), no. 3, 431–455.
[27] P. Seidel, π_1 *of symplectic automorphism groups and invertibles in quantum cohomology rings*. Geom. Funct. Anal. **7**(1997), 237–250.
[28] P. Seidel, *Lectures on four-dimensional Dehn twists*. In Symplectic 4-manifolds and algebraic surfaces, Lecture Notes in Mathematics, 1938, Springer, Berlin, 2008, pp. 231–267.
[29] S. Sternberg, *Minimal coupling and the symplectic mechanics of a classical particle in the presence of a Yang–Mills field*. Proc. Natl. Acad. Sci. USA **74**, 5253–5254.
[30] J. Zhang, *Symplectic structure perturbations and continuity of symplectic invariants*. Algebr. Geom. Topol. **19**(2019), no. 7, 3261–3314.

Center for Mathematical Analysis, Geometry and Dynamical Systems, Department of Mathematics, Instituto Superior Técnico, Avenida Rovisco Pais, 1049-001 Lisboa, Portugal
e-mail: sanjos@math.tecnico.ulisboa.pt

Utrecht Geometry Center, Utrecht University, Budapestlaan 6,3584 CD Utrecht, The Netherlands
e-mail: m.lourencohenriquesbarata@uu.nl

Department of Mathematics, University of Western Ontario, London, ON, Canada
e-mail: mpinson@uwo.ca

Department of Mathematics, Instituto Superior Técnico, Avenida Rovisco Pais, 1049-001 Lisboa, Portugal
e-mail: ana.alexandra.reis@tecnico.ulisboa.pt